# Development of Microfluidic Paper-Based Analytical Devices (µPADs) for Detection of Biomarkers


**Hokkaido University**
**Graduate School of Chemical Sciences and Engineering**

**Saeed Mohammadi**

**2016**

**Contents**

# Chapter 1. General introduction

## 1.1 Biomarkers

In 1998,[1] the National Institutes of Health Biomarkers Definitions Working Group defined a biomarker as "a characteristic that is objectively measured and evaluated as an indicator of normal biological processes, pathogenic processes, or pharmacologic responses to a therapeutic intervention." Biomarker measurements can help explain empirical results of clinical trials by relating the effects of interventions on molecular and cellular pathways to clinical responses. In doing so, biomarkers provide an avenue for researchers to gain a mechanistic understanding of the differences in clinical response that may be influenced by uncontrolled variables (for example, drug metabolism).[2] There are a variety of ways that biomarker measurements can aid in the development and evaluation of novel therapies.[3] In the initial investigations of therapeutic candidates in humans, biomarkers can provide a basis for the selection of lead compounds for phase 3 clinical trials.[4,5] Biomarkers contribute knowledge about clinical pharmacology and provide a basis for the designing of clinical trials that expeditiously and definitively evaluate safety and efficacy. Biomarkers provide information for guidance in dosing and minimize inter-individual variation in response. For example, rapid clearance of $^{99m}$Tc-sestamibi, a substrate for P-glycoprotein that is associated with multidrug resistance, has been shown to predict lack of tumour response

to adjuvant chemotherapy in some forms of breast cancer.[6] Biomarkers that represent highly sensitive and specific indicators of disease pathways have been used as substitutes for outcomes in clinical trials when evidence indicates that they predict clinical risk or benefit.

## 1.2 Microfluidic devices

### 1.2.1 Lab-on-a-chip

Microfluidic technology has evolved over the past few decades from a molecular analysis endeavour aimed at enhancing separation performance through reduced dimensions, into a diverse field influencing an ever-expanding range of disciplines.[7] Microfluidic techniques are being employed in chemistry, biology, genomics, proteomics, pharmaceuticals, biodefense, and other areas where its inherent advantages trump standard methodologies. From a biological standpoint, microfluidics seems especially relevant considering that most biological processes involve small-scale fluidic transport at some point. Example stem form molecular transfer across cellular membranes, to oxygen diffusivity through the lungs, to blood flow through microscale arterial networks.[8] Microfluidics can also provide more realistic in vitro environments for small-scales for several biological species of interest.[8] Figure 1.1 provides comparative number of publication concerning development of microfluidic devices

from 2000 to 2012.[9]

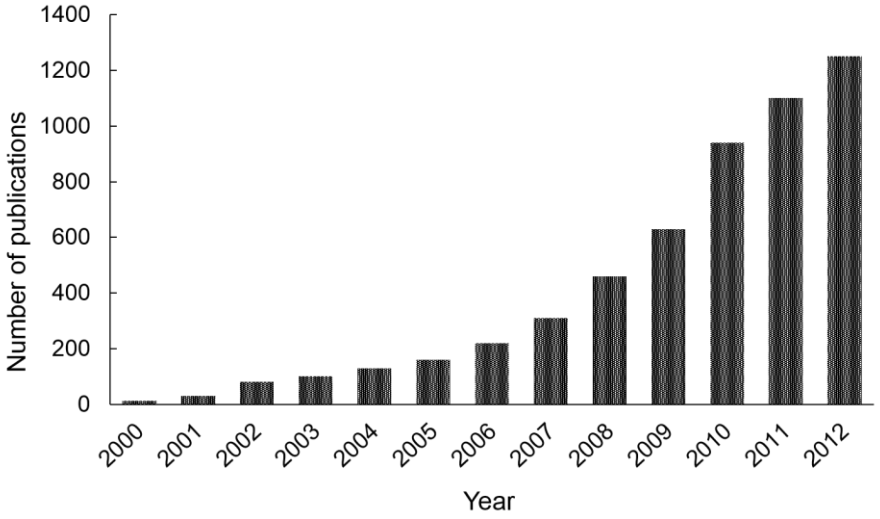


Figure 1.1 Research papers concerning development of microfluidic devices in years 2000-12.

### 1.2.2 Advantages of using microfluidic devices

Several measurements of analytical performance can be improved through miniaturization. Perhaps one of the most obvious advantages of smaller channel sizes is reduced reagent consumption, leading to less waste and more efficient assays.[8] Reduced reagent consumption becomes especially advantageous for many biological applications where reagents can be very expensive (e.g. antibodies), and sample volumes are often limited.[8] Additionally, the separation efficiency of chromatographic and electrophoretic

systems is proportional to the length of separation channel over its diameter ($L/d$).[8] Therefore long and narrow channels enable improved peak-peak resolution. Because they are so narrow, microfluidic channels also boast flows with very low Reynolds numbers: often $Re < 1$, meaning the flow is laminar.[8] Such laminar flows inhibit additional dispersion from affecting the band width of a separated plug. Diffusion, however, is more prominent at smaller scales and can be advantageous for mixing applications where, despite very laminar flow, mixing can occur solely via diffusion.[8] Narrow channels also dissipate heat more efficiently, allowing for higher electric fields in electrophoretic systems without adverse Joule heating effects on separation efficiency. As a result the assays will require less time as higher electric fields lead to faster separations. Microfluidic devices often achieve fluid transport with few mechanical components, which can significantly reduce an assay's complexity and power consumption over its macroscale counterpart. For example, electroosmosis is a process in which bulk electrolytic fluid in a channel is dragged via viscosity by migration ions near an inherently charged channel wall under the application of an electric field.[8] Electroosmosis allows for: a) bulk fluid "pumping" using only electric fields, thereby eliminating any moving parts, and b) a plug-like, non-parabolic fluid velocity profile that eliminates dispersion caused by parabolic pressure-driven flow. Bulk fluid transport

has also been demonstrated on microfluidic devices using other pumping techniques such as capillary wicking, evaporation, thermal gradients, and chemically-induced flow. With many conventional assays it is possible to integrate all analytical steps (sample loading, rinsing, reactions, separation, detection, etc.) into a single, fully-automated platform. Such integration reduces necessary human involvement, potential environmental contamination, and analysis time. With lab-on-a-chip devices, such integration can greatly reduce the cost per analysis while providing high throughput through parallelized or multiplexed devices.[8] They can also be potentially integrated into a portable, hand-held format for a variety of point-of-care (POC) applications where proper laboratory access is not available or rapid analysis time is required, including bedside patient care, military and border patrol, and global healthcare scenarios.

### 1.2.3 Disadvantages of using microfluidic devices

Early microfluidic systems predominantly used silicon as a substrate due to the wealth of existing fabrication techniques in microelectronic production.[8] Researchers used standard photolithography and etching processes to construct microfluidic channels of precise dimensions of silicon wafers. However, lithographic equipment is expensive and not accessible in resource limited setting. As research progressed,

however, the focus shifted from silicon to glass substrates. Glass presented a number of advantages over silicon. Perhaps its most obvious advantage is that glass is transparent, thereby allowing visualization of on-chip processes as well as simple detection for separation assays. In general, although the cost of glass and silicon wafers is about the same, glass became regarded as a simpler and more universal substrate for microfluidics. Using glass as a substrate has also some disadvantages include requiring a microscope to detect tracers in the glass channels and also it is expensive. For many applications, glass and silicon soon gave way to polydimethylsiloxane (PDMS), an elastomeric polymer used in everything from contact lenses to bathroom caulking. When cured, PDMS behaves like an elastic solid that maintains its molded structure. The use of PDMS for microfluidic applications was first presented by George M. Whiteside in the mid-1990's.[10,11] In this method the elastomeric monomer is poured over a master mold structure (typically a silicon wafer with an inverse photoresist structure of the channel geometry) and then cured. The cured structures can simply be peeled from the master and bonded to a planar substrate, forming the microchannel structures, which in most cases were irreversible. In addition, application of PDMS in microfluidic devices needs photolithographic equipment to create a mold. Furthermore, since PDMS is a hydrophobic polymer, flowing hydrophilic solution in channels made by PDMS needs

to apply an external force that usually is produced by a pump. So applying a more simple an affordable technique to fabricate microfluidic devices that is needless to external pump to flow the solutions was very desired.

### 1.3 Microfluidic paper-based devices

Recently, paper has been functionalised as a substrate to construct microfluidic devices for use in rapid diagnostic tests.[12] Figure 1.2 shows research papers concerning microfluidic paper-based analytical devices (μPADs) from 2008 to 2015. Patterning paper into regions of hydrophilic channels demarcated by hydrophobic barriers (or air) provides microfluidic devices that offer four basic capabilities on a single analytical device: (1) distribution of a sample into multiple spatially-segregated regions to enable multiple assays simultaneously (or replicates of an assay) on a single device; (2) moving the sample by capillary action (no pumps are needed); (3) compatibility with small volumes of sample, which is essential when sample size is limited (i.e. tears, saliva, urine from neonates and drops of blood from finger sticks); and (4) facile elimination of hazardous waste since the devices can be disposed of by incineration.[13]

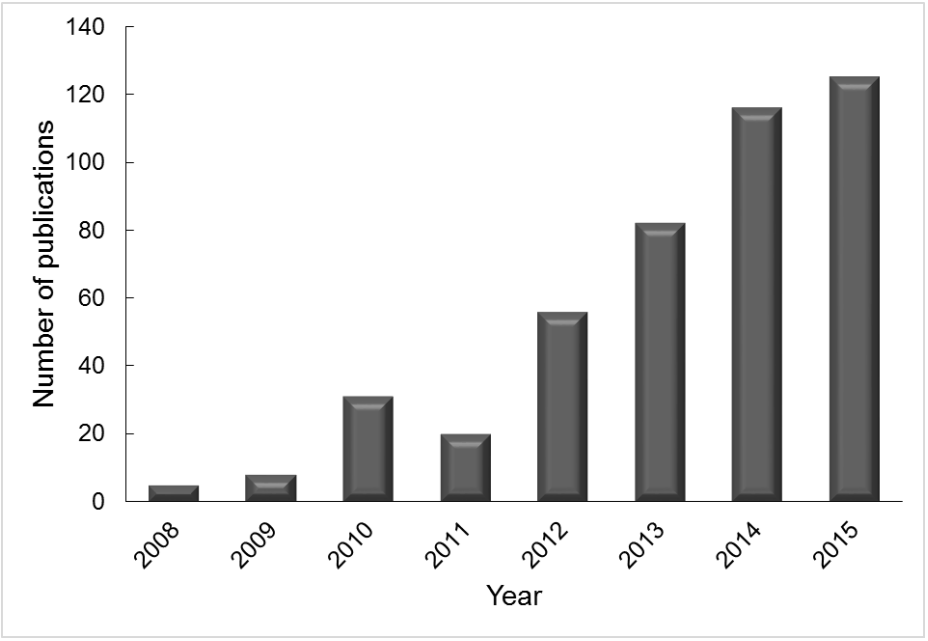


Figure 1.2 Research papers concerning μPADs in years 2008-15 (source: Web of Knowledge; data: May 6, 2016; key word: paper-based microfluidic devices).

## 1.4 Fabrication techniques of μPADs

In 2007, Martinez et al.[12] introduced a lithographic technique to create a microfluidic channel by using a hydrophobic photoresist, SU-8 polymer. The hydrophilic channel defined the liquid penetration pathway as it was confined within the hydrophobic walls. As the liquid was introduced to the hydrophilic channel, it moved through the paper matrix by capillary flow action. A three-branch tree pattern was lithographically patterned on the paper for the reaction site where different reagents were spotted for glucose and protein assays. This work was a major breakthrough that led to significant research growth in this field. It is attractive as it offers a simple and

relatively inexpensive alternative to existing technologies and is suitable for portable applications. Physical deposition of patterning agents such as wax,[14,15] polydimethylsiloxane,[16] and polystyrene[17] have been used to create paper devices by many research groups. One potential problem with the use of photolithography to create a microfluidic channel is that damage of the photoresist may occur during bending or folding. To overcome the problem introduced by photolithography, Bruzewicz et al.[16] demonstrated printing of elastomeric polydimethylsiloxane onto paper using a plotter. This allowed folding of the paper device without destruction of the channel. Moreover, the technique is highly reproducible and uses inexpensive materials, and is thus suited for even the most basic of research laboratories where microfluidic devices with feature sizes of ~1 mm are adequate. Solid wax patterns can be printed on the surface of paper followed by the use of a heat source such as an oven, hot plate or heat gun to melt the wax. Carrilho et al.[15] introduced the wax printing technique as a rapid, inexpensive and efficient process for prototyping a device in under 5 minutes. The technique is preferable for the fabrication of large quantities of sensors because fewer steps are involved in forming the hydrophobic barrier compared to photolithography. The heating process allows the wax to penetrate both vertically and horizontally within the paper matrix. Spreading of the wax vertically through the paper will effectively confine the

solution flow to the desired regions of the paper. However, due to the nature of the fibre matrix, the paper tends to align the wax in a horizontal, rather than vertical direction.[15] As a result, the wax spreads faster in the horizontal direction causing a wider line compared to the original width of the applied wax.[15] Therefore, the reproducibility of the fabrication method is highly dependent on the width of the wax line and the heating temperature. Approaches that involve selective removal or modification of the hydrophobic material after deposition have also been investigated in processes such as inkjet etching and plasma treatment. Abe et al.[18] formed hydrophilic channels by first hydrophobized paper by soaking it in a toluene solution containing poly(styrene). Subsequently, the hydrophilic region was defined by inkjet deposition of toluene to locally dissolve the poly(styrene) away from selected regions. Alternatively, Li et al.[19] used plasma treatment to chemically modify the surface. First they immersed filter paper into a hydrophobisation agent, alkyl ketene dimer (AKD), and then the hydrophobic AKD-treated paper was sandwiched between two metal masks and the hydrophilic channel for liquid transport was formed by plasma treatment of the functionalised paper. Wang et al.[20] demonstrated a tree-shaped paper for the semi-quantitative detection of protein. The filter paper was cut into a tree-shaped sheet with seven branches (3 mm × 45 mm) and a stem (8 mm × 55 mm). The design allows

uniform microfluidic flow along the multiple branches when the stem is placed into a wicking solution and spotted with the sample at the branch. Wang et al.[20] have demonstrated that calibration standards and measurements of an unknown can be performed at the same time using this tree structure. In a more defined approach, Fenton et al.[21] used a computer controlled X-Y knife plotter to form star, candelabra and other structures with the paper. They sandwiched the paper between vinyl and polyester plastic films in order to prevent evaporation and protect the surface from contamination and dehydration during the assay procedure. Shaping the paper by cutting has proven to be an easier technique compared to photolithography where multiple steps are required.

**References**


1. K. Strimbu and J. A. Tavel, Curr Opin HIV AIDS., 2010, 5, 463–466.
2. A. J. Atkinson Jr., W. A. Colburn, V. G. DeGruttola, D. L. DeMets, G. J. Downing, D. F. Hoth, J. A. Oates, C. C. Peck, R. T. Schooley, B. A. Spilker, J. Woodcock and S. L. Zeger, Clin. Pharmacol. Ther., 2001, 69, 89–95.
3. P. Rolan, Br J Clin Pharmacol., 1997, 997, 219–225.
4. J. W. Blue, and W. A. Colburn, Clin Pharmacol., 1996, 36, 767–770.
5. J. S. Fowler, N. D. Volkow, J. Logan, G-J. Wang, R. R. MacGregor, D. Schlyer, A. P. Wolf, N. Pappas, D. Alexoff, C. Shea, E Dorflinger, L. Kruchowy, K. Yoo, E. Fazzini, and C. Patlak, Synapse, 1994, 18, 86–93.
6. A. Ciarmiello, S. Del Vecchio, P. Silvestro, M. I. Potena, M. V. Carriero, R. Thomas, Clin Oncol., 1998, 16, 1677–1683.
7. J. C. McDonald, D. C. Duffy, J. R. Anderson and D. T. Chiu, Electrophoresis, 2000, 21, 27–40.
8. W. Tain and E. Finehout (eds), Microfluidic for Biological Applications, Springer, (2009).
9. E. K. Sackmann, A. L. Fulton and D. J. Beebe, Nature, 2014, 507, 181–189.

10. Y. Xia, E. Kim, X.-M. Zhao, J. A. Rogers, M. Prentiss and G. M. Whitesides, Science, 1996, 273, 347–349.

11. E. Kim, Y. Xia and G. M. Whitesides, Nature, 1995, 376, 581–584.

12. A. W. Martinez, S. T. Phillips, M. J. Butte and G. M. Whitesides, Angew. Chem., Int. Ed., 2007, 46, 1318–1320.

13. A. W. Martinez, S. T. Phillips, E. Carrilho, S. W. Thomas III, H. Sindi and G. M. Whitesides, Anal. Chem., 2008, 80, 3699–3707.

14. D. Zang, L. Ge, M. Yan, X. Song and J. Yu, Chem. Commun., 2012, 48, 4683–6485.

15. E. Carrilho, A. W. Martinez and G. M. Whitesides, Anal. Chem., 2009, 81, 7091–7095.

16. D. A. Bruzewicz, M. Reches, G. M. Whitesides, Anal. Chem., 2008, 80, 3387–3392.

17. J. Olkkonen, K. Lehtinen and T. Erho, Anal. Chem., 2010, 82, 10246–10250.

18. K. Abe, K. Suzuki and D. Citterio, Anal. Chem., 2008, 80, 6928–6934.

19. X. Li, J. F. Tian, T. Nguyen and W. Shen, Anal. Chem., 2008, 80, 9131–1934.

20. W. Wang, W. Y. Wu, W. Wang, J. J. Zhu, J. Chromatogr. A., 2010, 1217, 3896–3899.

21. E. M. Fenton, M. R. Mascarenas, G. P. López and S. S. Sibbett, ACS Appl. Mater. Inter. Faces, 2009, 1, 124–129.

# Chapter 2. Development of a new technique to fabricate microfluidic paper-based analytical devices (μPADs)

## 2.1 Introduction

Microfluidic paper-based devices (μPADs) have gained great attention in many fields such as point of care diagnosis,[1] environmental testing,[2,3] and food analysis.[4] These devices have numerous advantages, including low-cost fabrication, facile application, portability, and environmental compatibility.[5] μPADs systems have been applied for multiplex analysis in lab-on-a-chip devices.[6] μPADs also do not require external pumps and, by taking advantage of the wicking property of the paper, a complex flow design for various applications is possible.[7] Several low-cost methods for fabrication of μPADs have been reported including photolithography,[5] wax printing,[8,9] plasma treating,[10] and laser etching.[11] Various materials such as SU-8, poly(*o*-nitrobenzylmethacrylate) (PoNBMA), and octadecyltrichlorosilane (OTS) have been used to pattern hydrophobic barriers and form hydrophilic channels as μPADs on filter paper by photolithography. However, they can be easily damaged because of the flexibility of the support paper. Also, the photolithography method requires lithographic equipment and a rigid mask.[12] To reduce costs, several non-lithographic methods such as wax printing, plasma treating and laser etching have been reported for rapid, easy, and high resolution fabrication of μPADs. These methods generally need expensive equipment such as wax printers, plasma oxidizer and $CO_2$ lasers. This restricts their use

for fundamental research and for applications in ordinary laboratories, especially in less industrialized and resource-limited regions. Thus, cost-effective and simple methods to fabricate the μPADs without expensive equipment are highly desirable. An inkjet printing method as a simple and cost-effective alternative to expensive methods for patterning microstructures on filter paper has been developed.[13] Although this method is simpler, it is still limited by the requirement for the customized cartridges. Other fabrication methods such as silanization of filter cellulose[14] and printing of polymer solutions[15] have also been developed which efficiently form hydrophilic channels surrounded by hydrophobic barriers.

In this study, we purpose a low-cost, instrument free, and rapid fabrication method for μPADs; the method is suitable for employment in developing countries and resource-limited settings. We use a screen-printing method to pattern PDMS onto chromatography paper which produces hydrophilic channels with clear hydrophobic barriers. PDMS, a thermally curable polymer, is an excellent hydrophobic polymer which can penetrate the depth of the paper and form hydrophobic barriers that aqueous solutions cannot cross. Compared to the previously reported materials for screen-printing, PDMS is a thermo-curable inert polymer with proven compatibility for various chemical and biological assays under different pH, temperature, solvents, and

ionic conditions.[16] Screen-printing that we use in this research is also a low-cost and widely available printing technique in which a thick past ink is forced through a stencil attached to a woven mesh screen.[17] We have designed and fabricated several patterns for investing the performance of the fabrication method. We have also performed several colorimetric tests on fabricated µPADs for quantifying pH, glucose, and protein in both buffers and simulated urine samples.

## 2.2 Experimental

### 2.2.1 Fabrication of the µPADs

A WHT desktop printing table was purchased from Mino International Co., Ltd. (Tokyo, Japan). The WHT desktop printing table has three setting screws to allow movement of substrates in x and y directions. The printing table also has a vacuum pump to fix substrates on a board. Hydrophobic barriers as black zones on a white background were designed using Adobe Illustrator software (Adobe Systems, Inc.). A screen stencil (T-420 nylon mesh with ~35 µm pore size on an aluminium frame) was ordered from Unno Giken Co., Ltd. (Tokyo, Japan). Whatman chromatography paper 1# (200 × 200 mm) was purchased from GE Healthcare Life Sciences WhatmanTM (Tokyo, Japan). First, the patterned screen stencil was placed directly on a piece of chromatography paper, and PDMS was rubbed onto the surface of the screen stencil

using a squeegee, forcing PDMS past the pores of the woven mesh to form PDMS patterns in the paper (Figure 2.1). Afterwards, the patterned paper was cured in an oven set at 120 ˚C for 30 min. The PDMS-penetrated paper was ready for use after removing the paper from the oven and allowing it to cool quickly to room temperature.

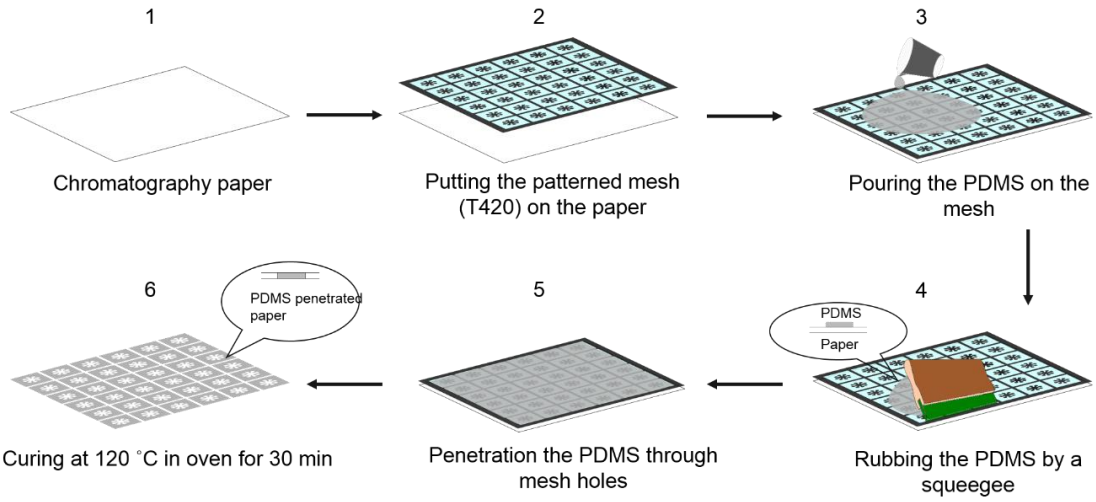


Figure 2.1 Schematic representation of PDMS-screen-printing for fabrication of the μPADs. (1), (2) Putting the screen directly on the chromatography paper surface; (3), (4) covering the screen with PDMS using a squeegee; (5) penetrating of the PDMS into the paper; (6) curing the PDMS-screen-printed paper in an oven set at 120 ˚C for 30 min.

### 2.2.2 Preparation of simulated urine solution

Lactic acid, calcium chloride, magnesium sulphate, ammonium chloride, sodium sulphate, sodium chloride and dipotassium hydrogen phosphate were purchased from Wako Pure Chemical Industries, Ltd. (Osaka, Japan). Potassium dihydrogen phosphate, urea and sodium bicarbonate were obtained from Kanto Chemical Co., Inc. (Tokyo,

Japan). Citric acid was purchased from Kishida Chemical Co., Ltd. (Osaka, Japan). Ultrapure water was obtained from a Millipore water purification system (18 MΩ·cm, Milli-Q, Millipore) and used for preparing all solutions and in all assays.

A simulated urine solution was prepared according to the literature.[18] In brief, 1.1 mM lactic acid, 2.0 mM citric acid, 25 mM sodium bicarbonate, 170 mM urea, 2.5 mM calcium chloride, 90 mM sodium chloride, 2.0 mM magnesium sulphate, 10 mM sodium sulphate, 7.0 mM potassium dihydrogen phosphate, 7.0 mM dipotassium hydrogen phosphate, and 25 mM ammonium chloride were dissolved in ultrapure water. The pH of the solution was adjusted to 6.0 using HCl (0.1 M).

2.2.3 Visualisation of different pH stock solutions

Thymol blue (TB), methyl red (MR), and sodium hydroxide (NaOH) were purchased from Wako Pure Chemical Industries, Ltd. Bromothymol blue (BTB), and phenolphthalein were purchased from Kanto Chemical Co. HEPES buffer was purchased from Dojindo Laboratories, Ltd. (Kumamoto, Japan). For visualisation of pH assay, a pH-responsive ink was prepared according to the literature.[13] Briefly, 0.5 mg of TB, 6 mg of BTB, 1.2 mg of MR, and 10 mg of phenolphthalein were dissolved in 10 mL of 95:5 (v/v) ethanol/water. Then, 0.01 M NaOH solution was added dropwise into the mixed indicator solution until the colour turned to light green. HEPES buffer (0.1

M) was used to make stock solutions and the pH of stock solutions were adjusted (2-9) by HCl or NaOH addition.

### 2.2.4 Glucose assay

Glucose and glucose oxidase were purchased from Wako Pure Chemical Industries, Ltd., and Sigma-Aldrich Co., Inc. (Tokyo, Japan), respectively. Potassium iodide was purchased from Kanto Chemical Co. The glucose stock solution (1 M) was diluted with the simulated urine solution and adjusted to concentrations of 0, 2.5, 5, 10, 20, 50, 100 and 500 mM. For the glucose assay, a 0.6 M solution of potassium iodide (15 µL) was first introduced into the auxiliary zone, followed by 1:5 horseradish peroxidase/ glucose oxidase solution (15 µL; 15 unit of protein per mL of solution). After exposing to air for 10 min at room temperature, 0.5 µL of different concentrations of glucose solutions were spotted onto eight separate sample zones.

### 2.2.5 Protein assay

BSA standard solution was purchased from Takara-Bio Co., Inc. (Shiga, Japan). Tetrabromophenol blue (TBPB) was purchased from Sigma-Aldrich Co., Inc. Citric acid was purchased from Hidex Co, Inc. (Osaka, Japan) and trisodium citrate was purchased from Wako Pure Chemical Industries, Ltd. BSA standard solution was diluted with ultrapure water to achieve the desired concentration (0, 2, 4, 6, 8, 10, and 20 µM). For

protein assay, 15 µL of a 250 mM citrate buffer solution (pH 1.8) was introduced into the auxiliary zone and exposed to air at room temperature for 10 min. Then, a 9 mM solution (15 µL) of TBPB in 95% ethanol was introduced onto the citrate buffer solution residue followed by exposing to air for another 10 min. Finally, 0.5 µL of the different concentrations of BSA solutions were separately spotted onto eight sample zones.

## 2.3 Results and Discussion

### 2.3.1 Evaluation of the appropriate channel width

To determine the minimum resolution of PDMS-Screen-Printing (PSP), we designed a pattern including different channel widths (Figure 2.2A). After fabrication, 7 µL of a 0.01 M fluorescein solution was dropped onto the paper to allow observation of the hydrophobic, hydrophilic, and wicking properties. Then fluorescence images were recorded by a fluorescence microscope (Keyence BZ-9000. Japan) (Figure 2.2B, C). In Figure 2.2B, hydrophilic channels (300, 400, and 500 µm) smaller than 600 µm were observed but solvent could not flow in them. The minimum width of the hydrophilic channel surrounded by printed PDMS barrier to deliver an aqueous sample was 600 µm but considering the wicking property, we recommend designing hydrophilic channels wider than 800 µm (Figure 2.2B). Furthermore, as shown in Figure 2.2B and Table 2.1, the printed channels were smaller than the pattern because after forcing the PDMS

through the mesh openings, there was slight leakage of the PDMS to the channel areas. In this method by making hydrophilic channels surrounded by a hydrophobic polymer (PDMS), no undesired leakage of PDMS into hydrophilic areas is expected. SEM images were obtained with a JEOL JSM-6390 scanning electron microscope and one is reproduced in Figure 2.2D. A recognizable borderline was seen between the bare and PDMS printed areas. These results have implications for some experiments where a minimum size of hydrophilic channels is required. For example, in order to decrease the amount of reagents, the minimum size of the mentioned features can be applied between sample zones where the wicking property is still suitable. Aqueous solutions have been found to flow better in smaller hydrophilic channels than in bigger channels in the µPAD system.[19] Also, long analysis times are not demanded in the µPAD system because no pump is needed to get fluid flows, and the µPAD can expedite solvent evaporation.[20] For these reasons, most 2D and 3D µPADs are going to be made smaller and smaller.[21] In the current study, for fabrication of the µPAD system, we used the 2 mm width hydrophilic channels as the basis.

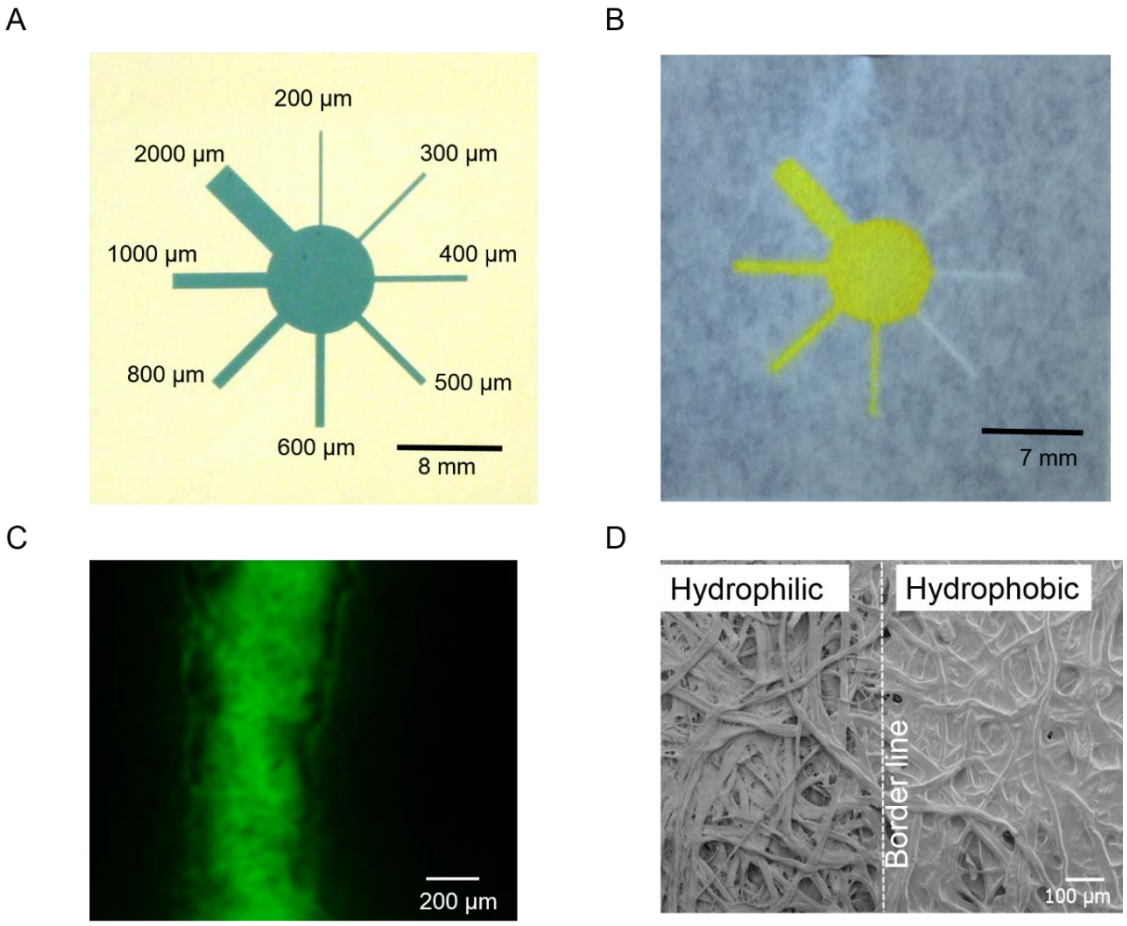


Figure 2.2 Evaluation of different channel widths. A) Patterned screen mesh for printing of different channel widths, B,C) comparison of the printed feature with the patterned screen and tracing the wicking property of them, D) SEM image of the bare (left) and PDMS printed paper (right).

Table 2.1 Comparison of the pattern and printed channel sizes

| Channel | Pattern size (mm) | Printed size (mm) |
|---|---|---|
| 1 | 2 | ~ 1.8 |
| 2 | 1 | ~ 0.8 |
| 3 | 0.8 | ~ 0.6 |
| 4 | 0.6 | ~ 0.4 |
| 5 | 0.5 | ~ 0.3 |
| 6 | 0.4 | ~ 0.2 |
| 7 | 0.3 | ~ 0.1 |
| 8 | 0.2 | 0 |

### 2.3.2 Optimization of the printing procedures and pH assays

A schematic representation of the μPAD fabricated by PSP was shown in Figure 2.1. Regarding optimisation of printed features and wicking property of μPADs, we designed a new pattern in order to investigate the performance of the fabrication method (Figure 2.3A).[8] For better visualisation of the pattern, carbon powder was dispersed in the PDMS solution. The μPAD for this, was arranged in an array of 8 sample zones with a 4 mm diameter and an auxiliary zone in the middle with an 8 mm diameter; this

provided simultaneous reaction in all sample zones (Figure 2.3B).[8] To evaluate the extent of PDMS spreading in the paper, the amount of PDMS and the frequency of rubbing were varied from 7-15 g and 1-3 times, respectively (Figure 2.3C). Then, 17 µL of a basic solution of phenolphthalein was dropped onto the auxiliary zone and leakage of the indicator solution was evaluated.

Temperature of the oven was set at 120 ˚C and the printed paper was cured for 30 min as described previously.[15] In order to prevent the cross contamination, no leakage of the indicator solution in the both front and back sides of the device must be achieved. At the onset of optimisation, we started with one rubbing application of 15 g PDMS. As shown in Figure 2.3C-I, this amount of PDMS was not enough to penetrate deeply into the paper cellulose structures and the indicator solution leaked from the printed pattern. During polymerization of the PDMS solution in the oven, PDMS penetrated slowly into the cellulose structures, and it was totally polymerized after 30 min; but that was before reaching the back side of the paper. On the other hand, almost half of the 15 g PDMS amount remained on the stencil after screen-printing. So, we decided to increase the frequency of rubbing to push the PDMS through the stencil into the cellulose structures. In the next attempt, we applied 15 g of PDMS with rubbing twice and basic solution of phenolphthalein was dropped as mentioned above (Figure 2.3C-II). The result for the

top side of the device was better than single rubbing but leakage of the indicator solution was still observed for the top and back sides. Furthermore, excess PDMS remained on the stencil. We increased the frequency of rubbing to three times (Figure 2.3C-III). This led to PDMS leaking into the hydrophilic areas in the back side. On the other hand, because the total size of the hydrophilic areas was decreased, cross contamination of the sample zones was observed in the top side. So to prevent the leakage, we decreased the amount of PDMS to 10 g and two rubbing times. This result is shown in Figure 2.3C-IV. For the back side, there was no leakage of the indicator solution but there was for the top side. Excess PDMS still appeared on the stencil, so we decided to decrease the amount of PDMS to 7 g and use three rubbing times (Figure 2.3C-V). Figure 2.3C-V shows good penetration of PDMS solution deep into the cellulose structures with no leakage of the indicator solution from the printed channels. We concluded that the optimum conditions for screen-printing of PDMS for this pattern were: 7 g PDMS, three rubbing times, and curing at 120 ˚C for 30 min.

In the current study, production of 36 µPADs by one screen-printing of PDMS solution on a piece of chromatography paper was possible. The cost for the paper and an aluminium frame is ~$8 (US) per 100 $cm^2$, so mass production of the µPADs is possible at a reasonable cost.

In order to investigate the performance of the µPADs, results for different pH solutions were obtained (Figure 2.3D). First, 0.5 µL aliquots of the different pH solutions (2-9) were separately spotted in the sample zones, and allowed to dry at room temperature for 10 min. Then, 15 µL of the pH-responsive ink was spotted in the auxiliary zone. From Figure 2.3D, we concluded it was possible to detect the pH of an unknown solution as a strip test, visually. Significantly, using the auxiliary zone in this pattern allowed the pH of samples from alkaline to acidic conditions, to be seen simultaneously. Furthermore, the cured PDMS was compatible with alkaline and acidic conditions because no leakage of solution was observed. This result showed the capability of the µPAD for assays in a pH range from 2 to 9.

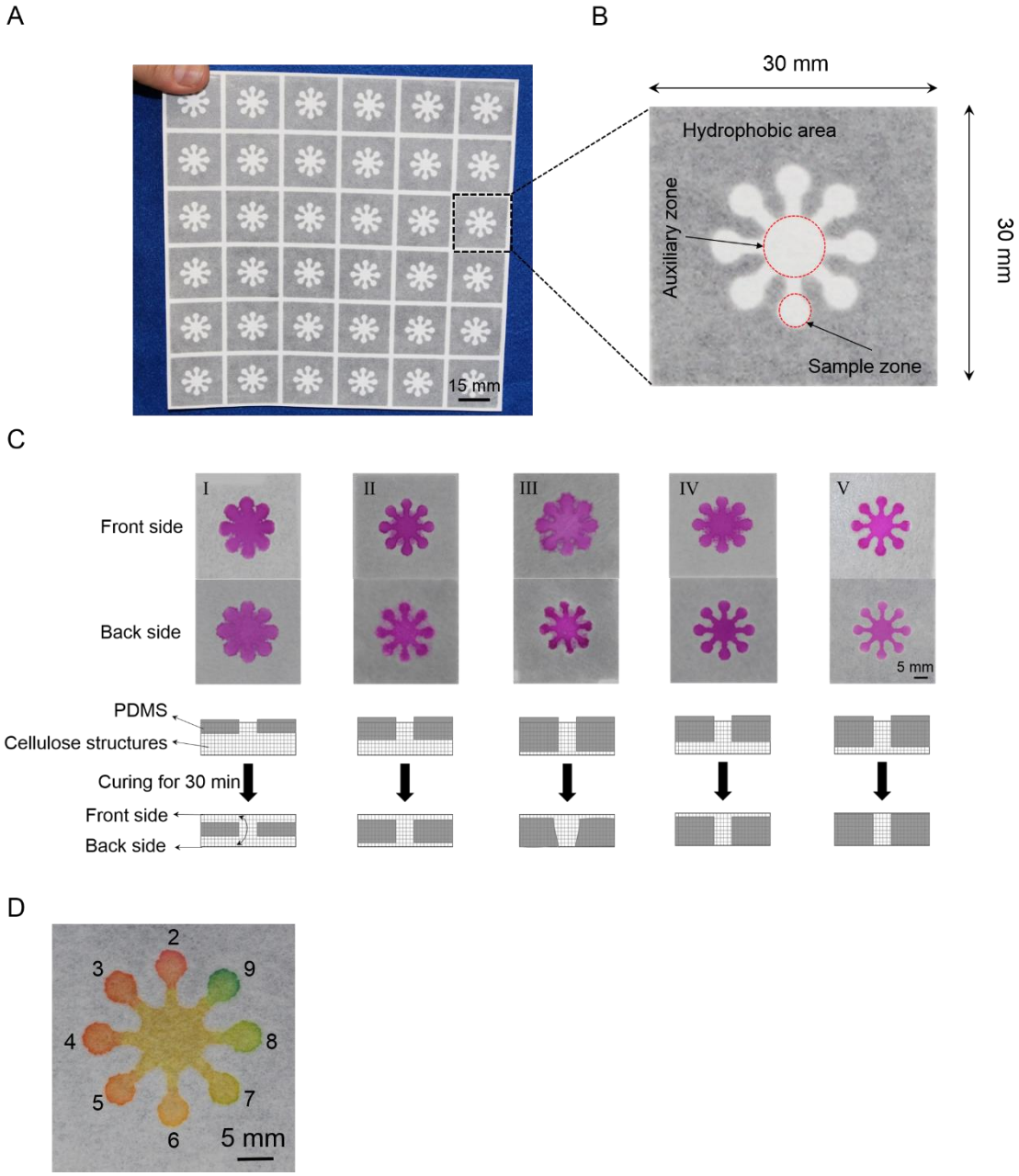


Figure 2.3 PDMS-screen-printing on a paper. A) Designing a new pattern (36 µPAD production one screen-printing). B) Details of each device. C) Optimising the printing procedures (All of devices were cured in an oven set at 120 ˚C for 30 min). I) Applying 15 g PDMS and rubbing once, II) applying 15 g PDMS and rubbing twice, III) applying 15 g PDMS and rubbing thrice, IV) applying 10 g PDMS and rubbing twice, V) applying 7 g PDMS and rubbing thrice. D) Results for different pH values (2 – 9). The colour of the sample zones changed from red at pH 2 to green at pH 9.

### 2.3.3 Optimization of pipetting volume

Because assay reagents are expensive, optimization of pipetting volume of solution into paper sample zones is important. Moreover, using a large volume of solution than the sample zones can contain can lead to cross contamination as a secondary problem. On the other hand, using a smaller volume of solution than the sample zones can contain can lead to miss-pipetting in multistep assays. 0.01 M fluorescein solution was traced using a fluorescence microscope as a model to investigate the optimum pipetting volume of solution in the sample zones. The investigation procedures included two simple steps: first different volumes of fluorescein solution (0.3-0.7 µL) were spotted in the sample zones and second, the fluorescence images of the sample zones were obtained with the fluorescence microscope. As shown in Figure 2. 4, 0.2, 0.3, and 0.4 µL volumes of the solution were not sufficient to fill all the sample zones. In addition for the reasons mentioned above, 0.6 and 0.7 µL volumes and more were not desirable. From these results, we considered 0.5 µL as the optimum pipetting volume in a sample zone (Figure 2. 4).

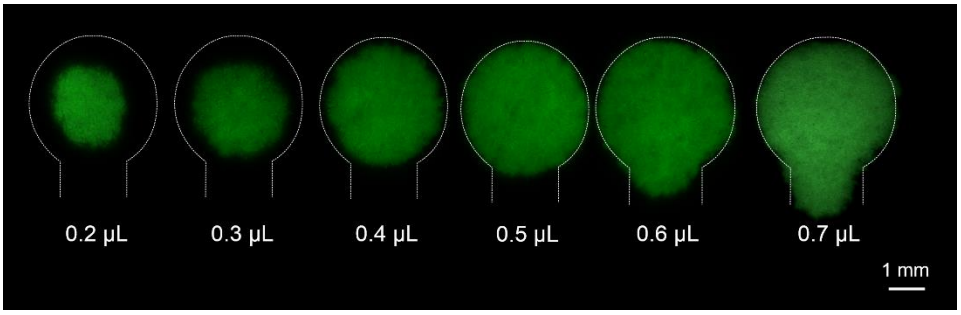


Figure 2. 4 Optimisation of pipetting volume in sample zones and sufficiency of solution immobilization.

### 2.3.4 Glucose and protein assays

µPADs, as mentioned earlier, have great potential for applications in various biochemical assays. Here we applied our method to two important biochemical assays: glucose and protein assays (Figure 2. 5). We prepared solutions with known concentrations of glucose in simulated urine and BSA standard solutions, and performed the colorimetric assays.[15] The results showed that the µPADs fabricated using the current method were applicable to determination of a 5 mM glucose in simulated urine which is adequate for detecting the critical concentration of glucose in diseases such as glucosuria.[22] This concentration was easily detectable by observation and could also be quantified using a hand hold camera and a simple image processing step.[18] The assay was repeated several times and reproducible results were achieved (Figure 2. 5A and B). We also tested a simple colorimetric assay for measuring protein concentration by our µPADs. Similar to the glucose assay, intensity of the colour was checked by observation

or by capturing an image and quantification of the signal using open source imaging software (ImageJ) (Figure 2. 5C and D). Limit of detection for BSA was 8 µM. The test can be applied to quantify protein in urine in nephrotic syndrome where, concentration of protein is higher than 35 µM.[18] In the current setting, detecting different concentration of protein ranging from 5 to 100 µM is possible.

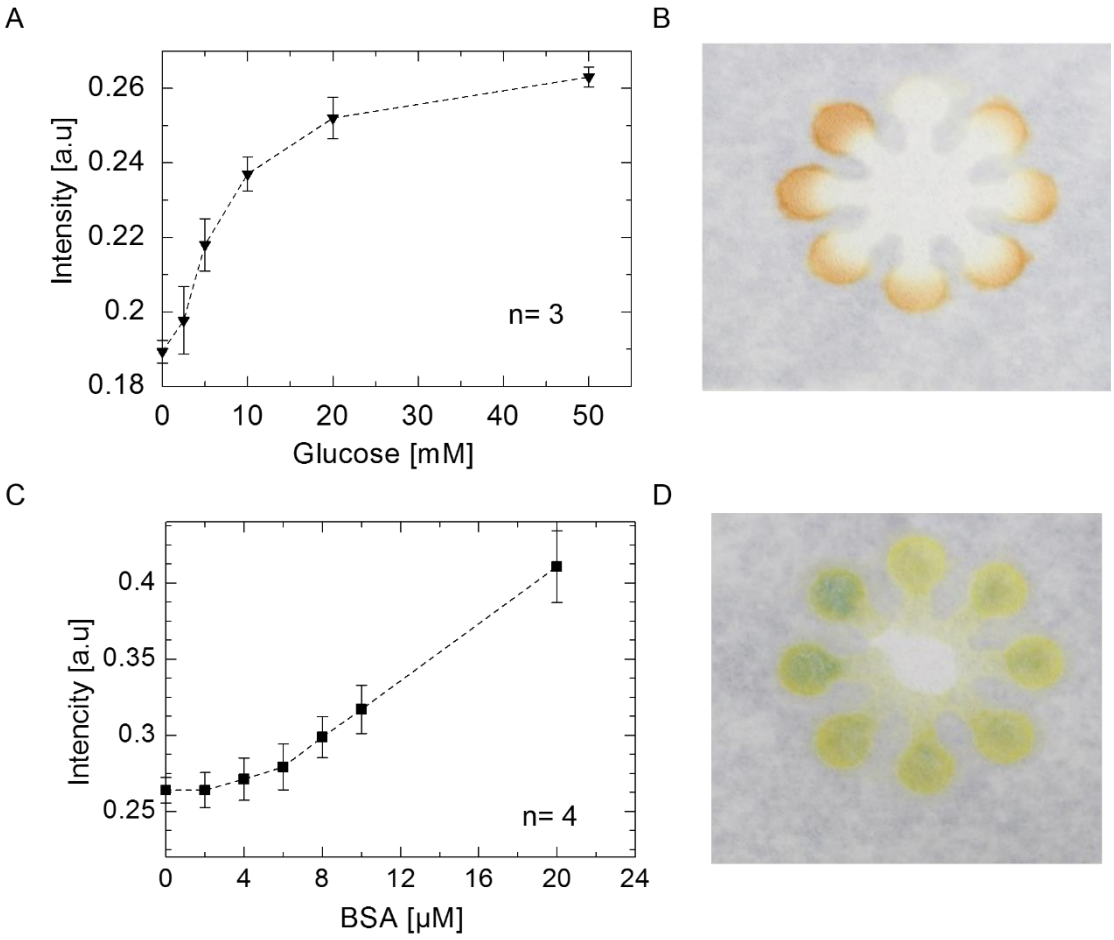


Figure 2. 5 Quantification and visualisation of glucose and protein assays. A, B) Quantification results (0-100 mM) and a µPAD used to visualise a positive test for glucose in simulated urine (0-500 mM), respectively. C, D) Quantification results (0-20 µM) and a µPAD used to visualise a positive test for BSA standard solution (0-30 µM), respectively. Each datum for the quantification results is the mean of three values for glucose and four for BSA; error bars represent the relative standard deviation of the measurements.

## 2.4 Conclusion

We used a simple, low-cost, and widely available screen-printing method to fabricate μPADs and we investigated the performance of this method using typical colorimetric detections for glucose and protein. We used PDMS to form clear hydrophobic borders on ordinary chromatography paper. High resolution micro channels were fabricated without using any printing machine such as a jet injection printer. We tested the fabricated μPADs for different chemical and biochemical sensing assays.

**References**


1. L. Tian, J. J. Morrissey, R. Kattumenu, N. Gandra, E. D. Kharasch and S. Singamaneni, Anal. Chem., 2012, 84, 9928–9934.
2. Y. Sameenoi, P. Panymeesamer, N. Supalakorn, K. Koehler, O. Chailapakul, C. S. Henry and J. Volckens, Environ. Sci. Technol., 2013, 47, 932–940.
3. M. M. Mentele, J. Cunningham, K. Koehler, J. Volckens and C. S. Henry, Anal. Chem., 2012, 84, 4474–4480.
4. J. C. Jokerst, J. A Adkins, B. Bisha, M. M. Mentele, L. D. Goodridge and C. S. Henry, Anal. Chem., 2012, 84, 2900–2907.
5. A. W. Martinez, S. T. Philips, M. J. Butte and G. M. Whitesides, Angew. Chem. Int. Ed., 2007, 46, 1318–1320.
6. A. W. Martinez, S. T. Phillips, G. M. Whitesides and E. Carrilho, Anal. Chem., 2010, 82, 3–10.
7. B. J. Toley, J. A. Wang, M. Gupta, J. R. Buser, L. K. Lafleur, B. R. Lutz, E. Fu and P. Yager, Lab Chip, 2015, 15, 1432–1444.
8. D. Zang, L. Ge, M. Yan, X. Song and J. Yu, Chem. Commun., 2012, 48, 4683–4685.

9. E. Carrilho, A. W. Martinez and G. M. Whitesides, Anal. Chem., 2009, 81, 7091–7095.

10. X. Li, J. Tian, T. Nguyen, and W. Shen, Lab Chip, 2008, 80, 9131–9134.

11. G. Chitnis, Z. Ding, C.-L. Chang, C. A Savran and B. Ziaie, Lab Chip, 2011, 11, 1161–1165.

12. S. Roy, J. Phys. D: Appl. Phys., 2007, 40, 413–426.

13. K. Abe, K. Suzuki and D. Citterio, Anal. Chem., 2008, 80, 6928–6934.

14. L. Cai, Y. Wang, Y. Wu, C. Xu, M. Zhong, H. Lai and J. Huang, Analyst, 2014, 139, 4593–4598.

15. D. A Bruzewicz, M. Reches and G. M. Whitesides, Anal. Chem., 2008, 80, 3387–3392.

16. E. Kim, Y. Xia and G. M. Whitesides, Nature, 1995, 376, 581–584.

17. S. Wang, L. Ge, X. Song, J. Yu, S. Ge, J. Huang and F. Zeng, Biosens. Bioelectron., 2012, 31, 212–218.

18. A. W. Martinez, S. T. Phillips, E. Carrilho, S. W. Thomas, H. Sindi and G. M. Whitesides, Anal. Chem., 2008, 80, 3699–3707.

19. E. Elizalde, R. Urteaga and C. L. A. Berli, Lab Chip, 2015, 15, 2173–2180.

20. K. M. Schilling, A. L. Lepore, J. a. Kurian and A. W. Martinez, Anal. Chem., 2012, 84, 1579–1585.

21. C. Renault, X. Li, S. E. Fosdick and R. M. Crooks, Anal. Chem., 2013, 85, 7976–7979.

22. J. Brodehl, B.S.Oemar, and P.F. Hoyer, Pediatr. Nephrol., 1987, 1, 502–508.

# Chapter 3. Novel concept of washing in µPADs

## 3.1 Introduction

The past few decades have seen the use of microfluidic paper-based analytical devices (μPADs) in bio and chemical sensing attract significant attention because the devices are inexpensive, portable, user-friendly, and environmentally compatible.[1,2] Inherent absorption of a liquid into a paper substrate by the action of capillary force is called the wicking property and it makes unnecessary the use of any external force such as a pump to get liquids to through the paper.[3] However, paper permeability drops during multistep assays such as enzyme linked immunosorbent assay (ELISA) due to saturation of paper pores by washing solutions.[4,5] Several detection methods have been implemented in μPADs have been reported such as colorimetric,[6] electrochemical,[7] fluorescence,[8] and chemiluminescence[9] detections. When a paper substrate is utilized for single step assays, for instance, colorimetric detection does not require any washing procedure,[8] whereas in multistep assays there is a necessity to wash out unbound agents from the paper in each step.[10] On the other hand, in ELISA on μPADs residual unbound antigen and antibodies after each step can lead to a high background signal.[11] In the previous reports, they directly added the washing solution to the sample zone and touched with a blotting paper but applying a constant flow of large amount of washing solution to remove unbound agents was difficult.[12, 13] Therefore, a suitable washing

technique for multistep assays in µPADs is highly desired. In this chapter, we describe a new washing concept for µPADs to eliminate unbound agents from deep in the paper substrate to achieve a lower background signal. A cartridge absorber was integrated with the paper substrate of the µPAD. The cartridge acts as a pores medium for the paper substrate in each step and can increase the permeability and flow of the washing solution through the cellulose structures of the substrate in multistep assays to wash out the residual unbound agents and improve the reproducibility and sensitivity. To confirm this idea, we made a polydimethylsiloxane (PDMS) holder including two channels using standard photolithography techniques; the holder is used to insert a cut chromatography paper as the paper substrate into the channels that are then sealed with adhesive tape. The cartridge absorber was prepared by putting a piece of blotting paper into a pipet tip such that it is connected to the paper substrate and it functions as an external pores medium.

## 3.2 Experimental

### 3.2.1 Fabrication of the PDMS holder

The holder was made of PDMS using standard photolithography techniques (Figure 3. 1). First of all, a silicon wafer was alternately cleaned with acetone and isopropanol

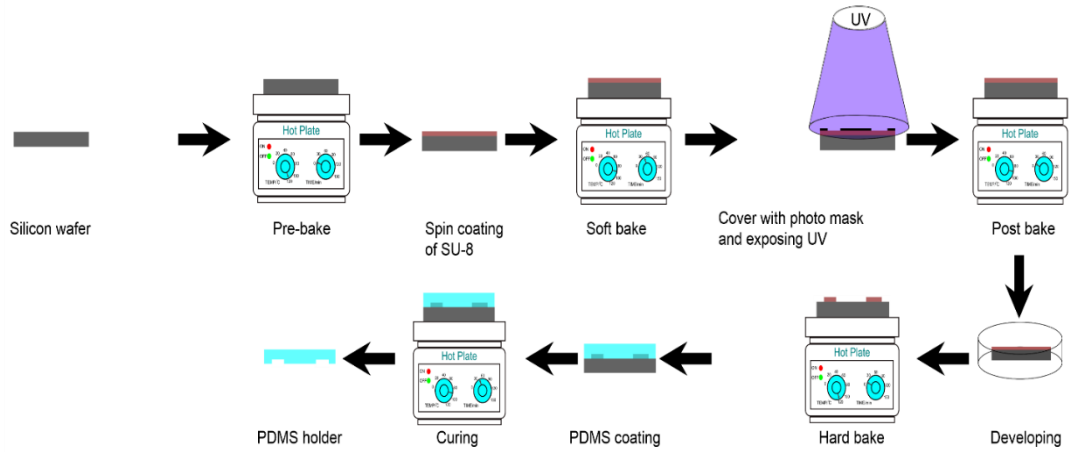


Figure 3. 1 Schematic of PDMS holder fabrication.

and baked at 120 ˚C. Then, SU-8 2075 was poured on the silicon wafer and it was spin coated at 1000 rpm to make a mold with a 240 µm thick wall. Next, the spin coated silicon wafer was cured as soft bake at 65 and 95 ˚C for 5 and 45 min, respectively. After cooling to RT, a photo mask was aligned on the coated wafer and UV light was exposed through the photo mask for 60 s. SU-8 photo resist was polymerized by UV irradiation and then cured as post bake at 65 and 95 ˚C for 1 and 10 min, respectively. Afterward, the silicon wafer was immersed for 10 min in SU-8 developer to remove non-polymerized SU-8, following by baking of the wafer and mold on a hot plate for 10 min at 150 ˚C. The cured SU-8 mold was used to make the PDMS holder.

### 3.2.2 Integration of the paper substrate into the PDMS holder

The holder had two channels of 240 μm in depth to integrate paper substrate (180 μm thickness) into the device. Holes were pierced into the holder for an inlet, an outlet, sample zones, and a tubing connection (Figure 3. 1). Whatman chromatography paper 1# (200 × 200 mm) was cut as the paper substrate using a craft cutter and inserted into the channels of the PDMS holder. After sealing the channels using adhesive tape, a silicone tube was connected to the PDMS outlet to connect with a syringe. The cartridge absorber (blotting paper) was arranged such that it was connected to the paper substrate. Figure 3. 2 shows schematic illustrations of the PDMS holder fabrication and a photograph of the μPAD.

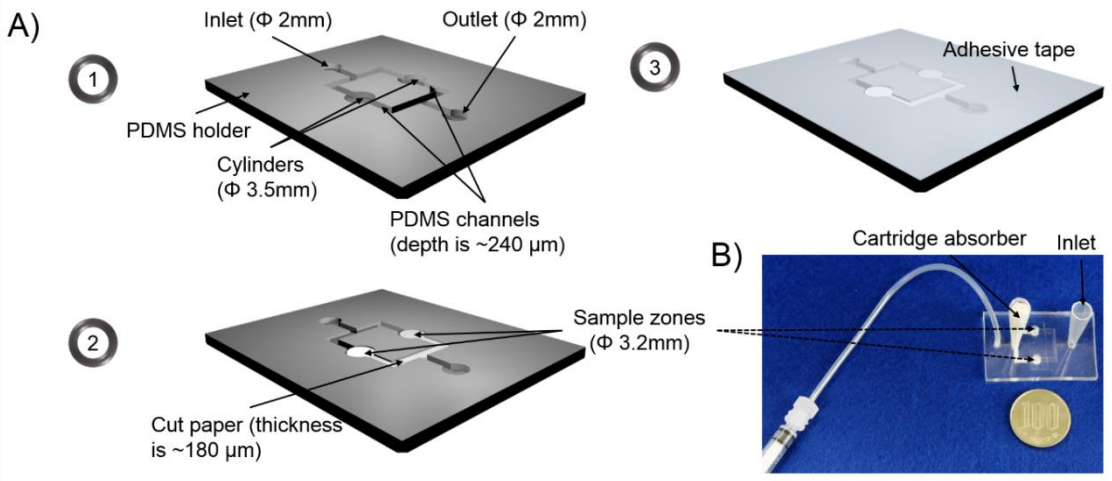


Figure 3. 2 A) Illustration of fabrication processes of the PDMS holder. (1) The PDMS holder had two cylinders where the sample zones of the paper substrate were integrated. (2) Paper substrate was inserted into the PDMS holder. (3) The holder was sealed using adhesive tape. B) Holes were pierced for an inlet, an outlet, the two sample zones, and a tubing connection.

### 3.2.3 Preparation of chitosan solution

Chitosan solution was prepared by adding 0.25 mg of flaked chitosan to hot HCl (70-80 ˚C). After cooling to RT, pH of solution was adjusted to 9 using NaOH and then filtered with a syringe filter (0.45 μm).[14]

## 3.3 Results and Discussion

### 3.3.1 Confirmation of immobilization of capture antibody cross-linked to chitosan

To confirm proper immobilization of capture antibody on the sample zones, we designed the following experiment. First, we pipetted 0.5 µL of fluorescein-labelled antibody on the sample zones and washed out the substrate paper applying 200 µL of 1% tween 20/PBS (Figure 3. 3B). Then fluorescence intensity was measured and compared with bare chromatography paper (Figure 3. 3A, B). As we expected, there was no significant difference between the results. Next, the surface of the sample zones was coated using 0.5 µL of the prepared chitosan, followed by air drying for 10 min. Afterward, 0.5 µL of labelled antibody was introduced into the chitosan-coated sample zones. After 30 min incubation, the sample zones were washed in the same way as mentioned above. Fluorescence intensity of sample zones significantly increased after coating the sample zones with chitosan (Figure 3. 3C). As the next demonstration, we used the same protocol as for the Figure 3. 3C demonstration, but before introducing the labelled antibody, chitosan was activated for 1h utilizing 2.5% glutaraldehyde in PBS. After washing the paper with ultra-pure water (200 µL), 0.5 µL labelled antibody was pipetted on the sample zones, followed by incubation for 30 min. The result of Figure 3. 3D confirmed that by coating the sample zones using 0.25 mg chitosan and then

activating with 2.5% glutaraldehyde/PBS, the captured antibody can be properly fixed in the sample zones.

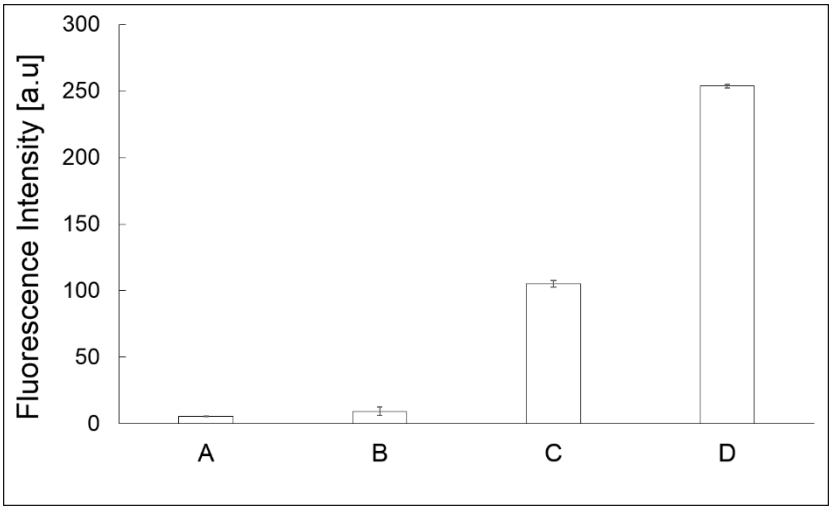


Figure 3. 3 Immobilization of capture antibody. Description of X axis results: A is the demonstration of intensity using bare chromatography paper, B is the demonstration using non-coated paper with chitosan, C is the demonstration using chitosan-coated paper, D is the demonstration using chitosan-coated paper and glutaraldehyde activation. Fluorescein-labeled antibody was introduced to the sample zones at the end of each demonstration and washed out using 200 µL of 1% tween 20/PBS.

### 3.3.2 Study of washing and blocking

To utilize the optimum volume of reagents in the sample zones without leakage to other parts of the paper substrate and to prevent miss-pipetting, optimization of pipetting volume is desired. We have mentioned the optimizing procedures in our previous study.[1] Briefly, as a model 0.01 M fluorescein solution was traced using a fluorescence microscope to investigate the optimum pipetting volume of solution in the sample zones. Different volumes of fluorescein solution (0.1-0.7 μL) were spotted in the sample zones and second, the fluorescence images of the sample zones were obtained with the fluorescence microscope (Figure 3. 4). From these results, we considered 0.5 μL as the optimum pipetting volume in a sample zone.

To examine washing, fluorescein-labelled antibody was pipetted into the sample zones and washed with different volumes of PBS buffer (50, 100, and 200 μL). Before washing the paper substrate, above of sample zone's cells which termed cylinders, were sealed by adhesive tape to prevent leaking of the washing solution. The washing solution was sucked out using the syringe connected to the outlet tubing until there was no solution touching the paper substrate and then sucking was stopped. We assumed that washing solution can move into the channels by the syringe sucking but when it touches the paper substrate it will move into those paper cellulose structures rather than keep

going into the channels because the PDMS channels are hydrophobic and the solution flows into the cellulose structures of paper by capillary force, naturally (Figure 3. 5A). We pipetted 0.5 μL of fluorescein-labelled mouse monoclonal antibody into sample zones and washed out the paper using PBS buffer. After washing, fluorescence images were captured using a fluorescence microscope and the average fluorescence intensity of each pixel was measured by AquaCosmos 2.6 software. Movies of the introducing and the washing out the fluorescence solution were shown in the Supporting Information. Fluorescence intensity gradually decreased with increasing volume of washing solution. Consequently, we found that applying 200 μL washing solution was enough to remove unbound agents and we could achieve essentially the same intensity as that of the bare paper (Figure 3. 5B). From these results, we judged our μPAD was able to eliminate unbound agents from the paper substrate by applying 200 μL of PBS solution with high reproducibility.

Blocking of paper substrates is one of the most challenging issues to eliminate bonding of agents to nonspecific areas in multistep immunoassays.[14] To achieve the best condition for blocking the paper substrate, different concentrations of bovine serum albumin (BSA) were studied to block non-specific adsorption to the sample zones from 0 to 1.5% in phosphate buffer saline (PBS) (Figure 3. 5C). Sample zones were covered

by 0.25 mg chitosan dissolved in HCl and then activated glutaraldehyde was pipetted on to the sample zones to bond to the antibodies (see Figure 3. 3).[15] Afterwards, the sample zones were blocked using different concentrations of BSA. Finally, the sample zones were washed by 0.05% Tween20/PBS. Then, labelled monoclonal mouse antibody was introduced to the sample zones, followed by incubation for 10 min. After incubation, the sample zones were rinsed with 0.05% Tween20/BSA in PBS (200 µL). According to the results, we concluded applying 1 to 1.5% BSA in PBS blocked the sample zones properly (Figure 3. 5D). Since residual BSA can physically degrade bonding of the capture antibody and antigen,[16] applying a suitable concentration of BSA for blocking the paper substrate is important. For this reason, we recommend 1% BSA to block the sample zones.

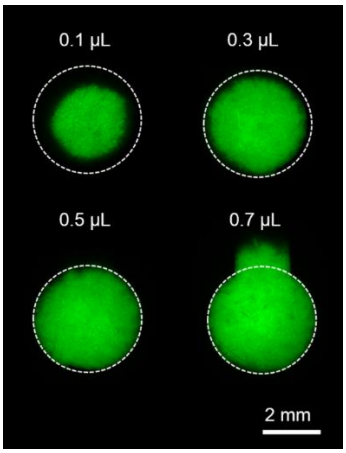


Figure 3. 4 Optimization of pipetting volume.

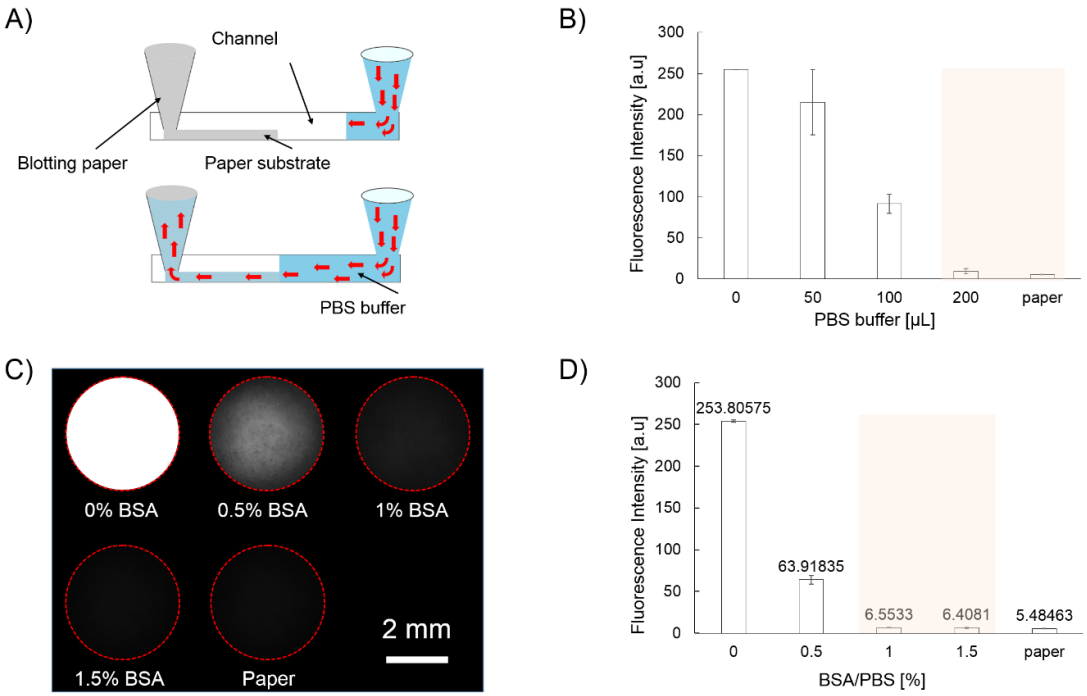


Figure 3. 5 Experiment to confirm washing and blocking of the paper substrate. A) Illustration of behaviour of solution in one channel after coming into contact with the paper substrate. B) Optimization of washing procedure (proper volumes of washing solution to remove unbound agents are highlighted). C) Fluorescence images of sample zones after applying different concentrations from 0 to 1.5% of BSA in PBS. D) Demonstration of proper amount of BSA in PBS to block the sample zones in order to prevent non-specific bonding of agents (recommended amount of BSA in PBS: 1 to 1.5 %).

### 3.3.3 CRP detection

As an assay model, we applied the washing technique to a sandwich assay of C-reactive protein (CRP).[17] After assembling the device including the PDMS holder and paper substrate using adhesive tape, we activated the sample zones using chitosan and glutaraldehyde. Next, 0.5 µL of anti-CRP mouse monoclonal antibody (100 µg $mL^{-1}$) as a capture antibody was introduced to the sample zone, followed by incubation for 30 min. To remove the unbound capture antibodies, 200 µL of 0.05% Tween20/BSA in PBS was applied using the washing technique. The sample zones with the capture antibody were blocked using 1% BSA/ PBS for 15 min and washed with 200 µL 0.05% Tween20/BSA in PBS. Various concentrations of CRP from 0 to 50 µg $mL^{-1}$ were introduced into the sample zones and incubation was done for 20 min. After washing as in the previous step, 0.5 µL of rabbit polyclonal antibody was added to each sample zone and this was incubated for 1 min followed by another washing as before. Finally, goat labelled polyclonal antibody was added to each sample zone and this was incubated for 1 min followed by washing with 200 µL 0.05% Tween20/BSA in PBS, three times (Figure 3. 6A, B). Fluorescence images were captured using the fluorescence microscope. Removing unbound agents in each step, relying on the spontaneous capillary force of the paper substrate lead to detection of CRP with a limit

of detection of 5 µg $mL^{-1}$ with a small standard deviation (0.098) and high reproducibility (Figure 3. 6C, black curve). Furthermore, we detected CRP using the conventional technique of washing µPADs. In the conventional technique, µPADs are touched with a piece of blotting paper during washing steps in multistep assays to remove unbound agents.[15] However, because of low permeability after each washing step, applying same volume of washing solution as mentioned above (200 µL) was impossible. We fabricated a µPAD according to our previous report using screen-printing of PDMS on chromatography paper[1] and carried out the same assay protocol as mentioned above to detect CRP (Figure 3. 6C, red curve). As shown in Figure 3. 6C, the developed concept of washing significantly decreased the background signal. In addition, in the conventional technique, there was a slightly higher signal for 5 µg $mL^{-1}$ CRP than the control (0 µg $mL^{-1}$) that was attributed to low permeability of the paper substrate during the assay. On the other hand, a significantly higher signal for 5 µg $mL^{-1}$ CRP than the control using the current washing technique provided proper permeability of the paper substrate such that large amounts of antigen and antibodies were bound deep in the paper. Furthermore, increasing the porosity by allowing more reagents to permeate through the depth of the paper led to an enhanced detection signal at higher concentrations of CRP.

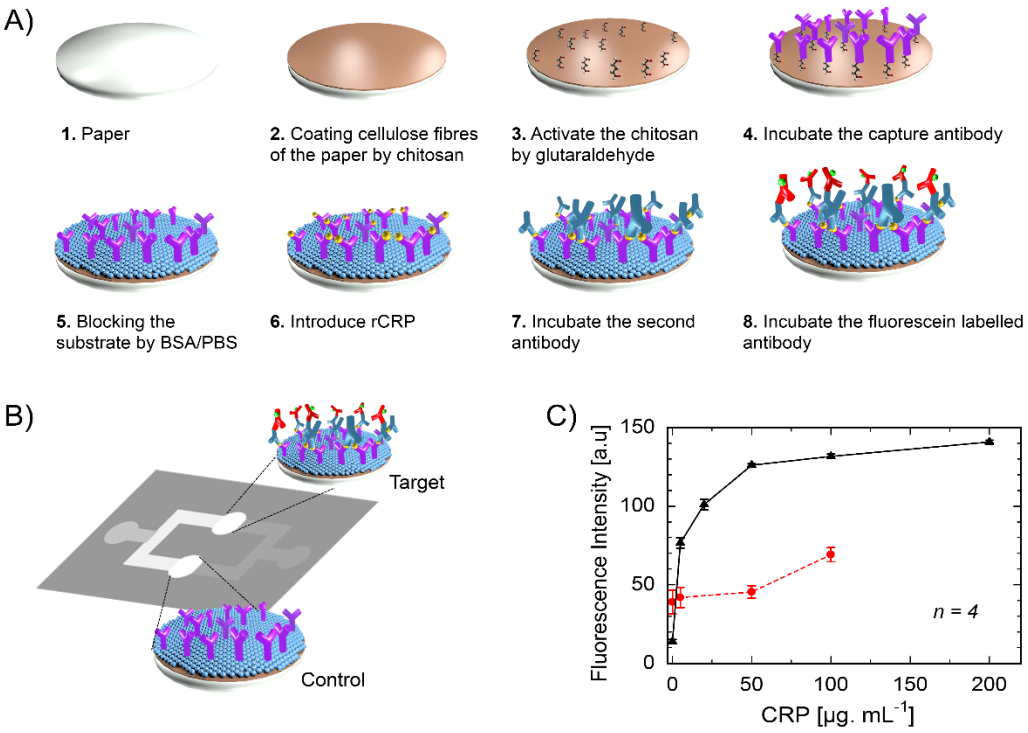


Figure 3. 6 A, B) Schematic drawings of CRP immunoassay. C) Standard curves for CRP assay. Black is the standard curve obtained by this study for the novel washing technique and red is the standard curve obtained by the conventional technique of washing the paper substrate.

## 3.4 Conclusion

In this study, we considered a new concept for washing of µPADs relying on spontaneous capillary force of the paper substrate. We demonstrated that increasing the permeability of the paper substrate used for multistep assays led to proper removal of unbound agents and decreased the background signal. As an assay model, CRP was detected with the limit of detection of 5 µg $ml^{-1}$. In comparison with the conventional washing technique, the new method developed here for washing of µPADs provided significantly higher sensitivity and reproducibility. By exploiting our washing concept, researchers can be closer to applying µPADs for multistep assays with a low background signal.

**References**


1. S. Mohammadi, M. Maeki, R. M. Mohamadi, A. Ishida, H. Tani and M. Tokeshi, Analyst, 2015, 140, 6493–6499.
2. L. S. A. Busa, M. Maeki, A. Ishida, H. Tani, M. Tokeshi, Sens. Actuators B, 2016, 236, 433–441.
3. R. Masoodi and K. M. Pillai, AIChE J., 2010, 56, 2257–2267.
4. F. T. Carson, B.S.J. Res.,1934, 12, 567-608.
5. L. Pal, M. K. Joyce, P. D. Fleming and D. S. Law, Tappi J., 2006, 5, 10-16.
6. A. W. Martinez, S. T. Phillips, M. J. Butte and G. M. Whitesides, Angew. Chem. Int. Ed., 2007, 46, 1318–1320.
7. H. Liu, Y. Xiang, Y. Lu and R. M. Crooks, Angew. Chem. Int. Ed., 2012, 51, 6925–6928.
8. H. Liu and R. M. Crooks, J. Am. Chem. Soc., 2011, 133, 17564–17566.
9. L. Ge, S. Wang, X. Song, S. Ge and J. Yu, Lab Chip, 2012, 12, 3150–3158.
10. S. Wang, L. Ge, X. Song, J. Yu, S. Ge, J. Huang and F. Zeng, Biosens. Bioelectron., 2012, 31, 212–218.
11. A. K. Yetisen, M. S. Akram and C. R. Lowe, Lab Chip., 2013, 13, 2210–2251.
12. J. Liang, Y. Wang and B. Liu, RSC Adv., 2012, 2, 3878–3884.

13. G. A. Posthuma- Trumpie, J. Korf and A. Van Amerongen, Anal Bioanal Chem., 2009, 393, 569–582.

14. J. E. Schonhorn, S. C. Fernandes, A. Rajaratnam, R. N. Deraney, J. P. Rolland and C. R. Mace, Lab Chip., 2014, 14, 4653–4658.

15. D. Zang, L. Ge, M. Yan, X. Song and J. Yu, Chem. Commun., 2012, 48, 4683–4685.

16. R. Kaur, K. L. Dikshit and M. Raje, J. Histochem. Cytochem., 2002, 50, 863–873.

17. M. Ikami, A. Kawakami, M. Kakuta, Y. Okamoto, N. Kaji, M. Tokeshi and Y. Baba, Lab Chip., 2010, 10, 3335–3340.

# Chapter 4. Development of microfluidic devices for detection of cCys-C

## 4.1 Introduction

Chronic kidney disease (CKD) is diagnosed commonly in cats specially older cats.[1] Several literatures have shown 53% of cats ≥7 years old and 69-81% of cats ≥10 years old were diagnosed with CKD.[2] Causes of CKD are widely heterogeneous and rarely identified however the most common sign is tubulointerstitial nephritis with variable degrees of fibrosis. According to outline by the International Renal Interest Society (IRIS), CKD is diagnosed as staging (I-IV) and sub-staging based on concentration of serum and proteinuria, respectively.[3] Expensive diagnostic procedures of renal dysfunction in pets, often lead to major surgeries and so unfortunate in most cases dying. Because in patients with chronic kidney disease there is a high risk of progression to irreversible renal damage, especially in a more advanced stage, it is extremely needed for early and specific detection of kidney dysfunction in both humans and pets. Hence, development of a cheap technique to detect minor renal function in pets is desirable. Despite various techniques have been developed to explore symptoms of renal failures in human serum, but determination of them in pets still need to more consideration. Glomerular filtration rate (GFR) is generally accepted as the best overall index of renal function and is therefore an important marker for renal disease.[4] Although insulin clearance is considered to be the gold standard for the measurement of GFR, its use is

limited in clinical practice as it is difficult to obtain, requires constant rate infusions and is difficult to measure accurately. In clinical practice, serum creatinine (SCr) is the most commonly used parameter for monitoring renal function. When more precise information on renal function is needed, a 24h urine collection is often performed to calculate the creatinine clearance (CrCl).[5] However, there are some shortcomings to the use of this parameter. Many factors, such as age, gender, muscle mass, drug and protein intake can influence SCr, leading to an inaccurate estimation of renal impairment. Normal SCr may be observed in individuals with significantly impaired GFR.[6,7] Moreover, in unstable, critically ill patients, acute changes in renal function can make real-time evaluation of GFR using SCr difficult. On the other hand, CrCl requires urine collection over a 24 h period with a steady-state situation.[8] Cystatin C (Cys-C) is a 13 kDa cysteine proteinase inhibitor, produced and secreted by almost all nucleated cells at a constant rate, freely filtered by the glomeruli, reabsorbed, and catabolized in the proximal tubular cells but not secreted by the tubules.[9] Due to its constant rate of production, its serum concentration is determined by glomerular filtration.[10] Moreover, its concentration is not influenced by infections, liver diseases or inflammatory diseases. Therefore, a growing number of clinical studies on patients with a variety of renal pathologies have indicated that Cys-C is superior or at least equivalent to SCr level as

an index of GFR.[11] In the present chapter, the value of serum cat Cys-C (cCys-C) level as a marker for monitoring kidney function in cat was prospectively evaluated using conventional 96-wall microtiter plate and immuno-pillar chip which is developed by our group previously.[12- 14] In addition a new system has been developed to detect cCys-C using μPADs.

## 4.2 Experimental

### 4.2.1 Microtiter plate

#### 4.2.1.1 Preparation the solutions

Enzyme linked immunosorbent assay (ELISA) kit for cat cystatin C (cCys-C) was purchased from Nippro, Osaka, Japan. The kit involved; a 96 well microtiter plate included capture anti-cCys-C, 0.5 mL labelling anti-cCys-C (C1), different concentrations of cCys-C (1 mL), sample diluent solution (60 mL), 15 mL enzyme labelling solution (C2), substrate for the enzyme (15 mL), stop solution (15 mL), and washing buffer solution (50 mL). First of all we have to dilute the washing buffer solution 40 times and C1 30 times with ultrapure water and C2, respectively.

#### 4.2.1.2 cCys-C assay using the 96 well microtiter plate

A cCys-C ELISA kit from Nipro Co., Ltd., was used, and a control test in a microtiter plate was carried out based on the manufacturer's instructions. First, 100 µL of cCyc-C solutions with concentrations from 0 to 50 ng $mL^{-1}$ were pipetted into a 96-well microtiter plate, which was pre-coated using anti-cCys-C antibody. Then the plate was incubated at 37 ˚C for 1 h. Afterwards, each well of the plate was rinsed 7 times with 350 µL of the washing buffer. Next, 100 µL of the horseradish peroxidase-labelled anti-cCys-C antibody was pipetted into each well and the mixture was incubated for 30

min at 37 ˚C. Then, each well was rinsed 9 times with 350 µL of the washing buffer. Afterwards, 100 µL of the substrate solution consists of 3,3',5,5'-Tetramethylbenzidine and hydrogen peroxide was pipetted into each well and incubated for 30 min at room temperature in the dark. Finally, the kit stop solution was pipetted into each well (100 µL) and the absorbance at 450 nm was measured using a microplate reader (Model Sunrise-Basic Tecan, Tecan Japan Co., Ltd, Kawasaki, Japan) within 30 min.

4.2.2 Immuno-pillar chip

4.2.2.1 Incubation of the capture anti-cCys-C on affinity microbeads

10 mg affinity microbeads, 27.67 µL of capture antibody, and 500 µL of a protein fixative solution were add to a 1.5 mL microtube and mixed for 4h at 37 ˚C. Then the microtube was centrifuged at 5000 g for 60 seconds at 25 ˚C and the fixative solution was removed from the microtube. The affinity microbeads were washed by adding 1 mL of 0.01% Tween 20/PBS and centrifuging again as mentioned above to remove washing solution from the microbeads, alternatively (X4). Then 500 µL of an inactivation solution was added to the microbeads and incubate for 1h at room temperature. Afterwards, the microtube was centrifuged at 5000 g for 60 seconds at 25 ˚C and the inactivation solution was removed from the microtube. The affinity microbeads were washed as mentioned above (X3). Finally the washing solution was removed and the

microbeads were dried for 1h at 37 ˚C.

4.2.2.2 Fabrication of immuno-pillars

Figure 4. 1 illustrates the fabrication procedures for immuno-pillars. First, the beads which were used to form the immuno-pillars were prepared. An affinity bead kit (Catalog No: BS-X9905) was purchased from Sumitomo Bakelite Co., Ltd., Osaka, Japan. 10 mg of the affinity beads (5 μm in diameter) and 150 μg $mL^{-1}$ anti-cCys-C (mouse monoclonal IgG) in the coupling buffer were transferred to a microcentrifuge tube and incubated for 4h at 37 ˚C in a rotary shaker. Then, the microtube was centrifuged at 5000 g for 60 s at 25 ˚C and the supernatant was discarded. The beads were washed 3 times with wash buffer (0.01% Tween 20/PBS) and centrifuged as mentioned above to remove the washing solution. Then 500 μL of blocking buffer was added to the beads and this was incubated for 1 h at room temperature. After that, the microtube was centrifuged at 5000 g for 60 s at 25 ˚C and the supernatant was discarded. The beads were washed 3 times with PBS buffer as mentioned above. Finally, the washing solution was discarded and the beads were dried for 1 h at 37 ˚C.

Next, the microchannels in which the immuno-pillars were to be fabricated were prepared. Cyclic olefin polymer (COP) chips, each with 40 microchannels, were purchased from Sumitomo Bakelite Co., Ltd. A photocrosslinkable prepolymer (Catalog

No: ENTG3800) and a photoinitiator (Catalog No: PIR-1) were purchased from Kansai Paint Co., Ltd, Osaka, Japan. A mixed solution of PBS buffer, the photocrosslinkable prepolymer, and the photoinitiator was prepared in the volume ratio of 150: 25.5: 12, respectively. 125 µL of this solution was added to the dried beads, followed by gentle mixing. Then the suspension solution of the beads was introduced into the microchannels on a COP chip. Next, the chip was covered with a photomask which had five open areas where pillars (200 µm in diameter) were made in each microchannel and the chip was irradiated with ultra violet light 60 s. After removing the photomask, the channels with the immuno-pillars were washed with 1% BSA/PBS and the chip was stored at 4 ˚C prior to use.

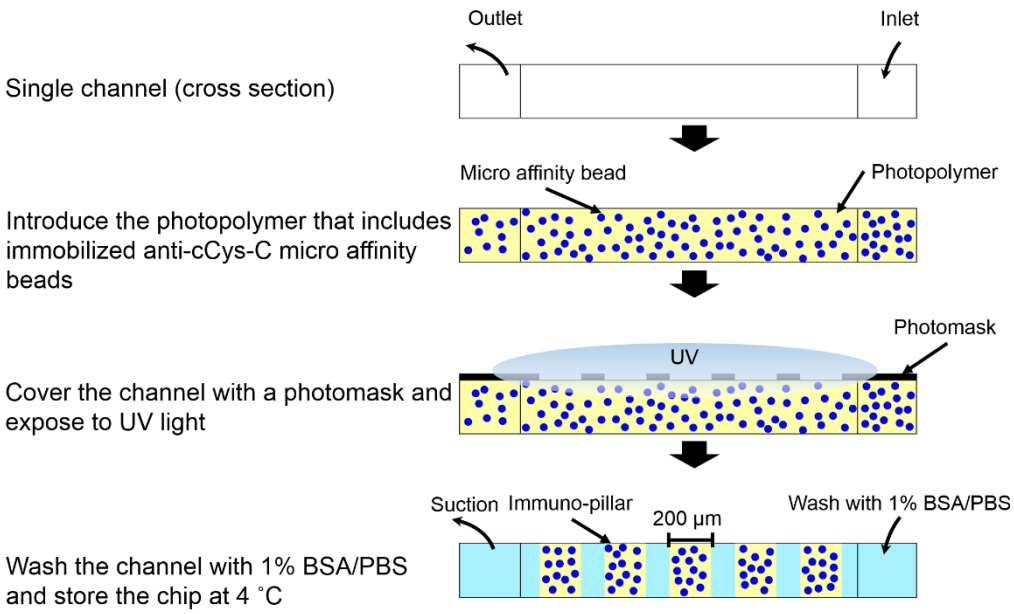


Figure 4. 1 Illustration of fabrication of immuno-pillars

#### 4.2.2.3 cCys-C assay using the immune-pillar chip

The procedure for the cCys-C assay was as follows. All the channels with the micro immuno-pillars were washed 5 times with 0.01% Tween 20/PBS. Then, 7 different concentrations of cCys-C (Nipro Co., Ltd., Osaka, Japan) from 0 to 50 ng $mL^{-1}$ were introduced into the channels separately and each solution was incubated for 10 min at room temperature. Afterwards, the channels were rinsed with PBS buffer 5 times. Fluorescence-labelled anti-cCys-C (mouse monoclonal IgG) was prepared using the Zenon® Alexa Fluor® 488 rabbit IgG labelling kit (Thermo Fisher Scientific Co. Ltd, Yokohama, Japan). This anti-cCys-C solution was introduced into the channels and was incubated at room temperature for 10 min in the dark. Finally, the channels were rinsed with PBS buffer 5 times. Fluorescence images were captured by a fluorescence microscope (ECLIPSE Ti-U, Nikon Co., Ltd., Tokyo, Japan) equipped with a CCD camera (ORCA-R2, Hamamatsu Photonics K. K., Hamamatsu, Japan) and the intensity was measured using AquaCosmos software (Hamamatsu Photonics K. K.). Figure 4. 2 is a schematic of cCys-C assay in a channel of immuno-pillar chip.

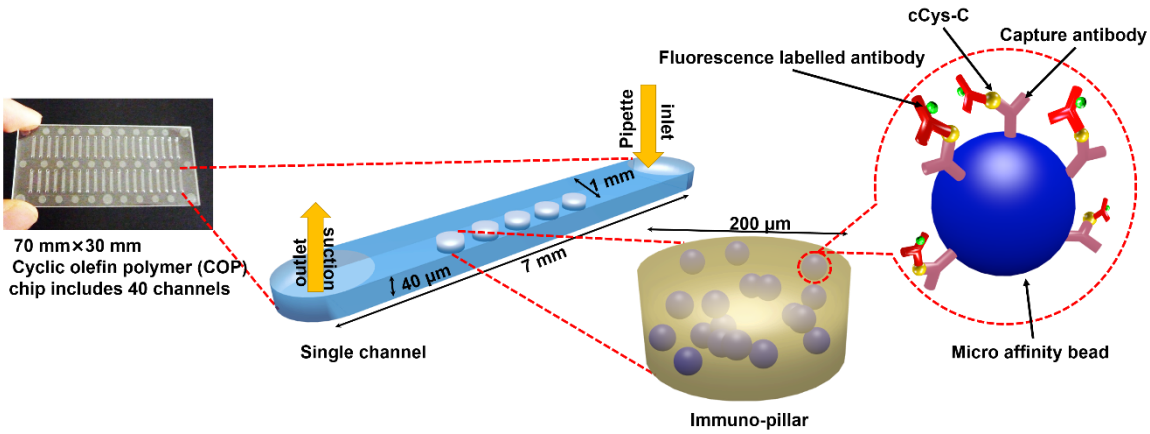


Figure 4. 2 Schematic of cCys-C assay in a channel of immuno-pillar chip.

### 4.2.3 Develop a new system to detect cCys-C using iµPADs

#### 4.2.3.1 Fabrication of a iµPAD

Briefly, the holder was made of PDMS using standard photolithography techniques (As mentioned earlier in chapter 3). The holder had four channels of 240 µm in depth to integrate paper substrate (180 µm thickness) into the device. Holes were pierced into the holder for an inlet, an outlet, and sample zones. Whatman chromatography paper 1# (200 × 200 mm) was cut as the paper substrate using a craft cutter and inserted into the channels of the PDMS holder. The cartridge absorbers (blotting paper) were arranged such that it was closed to the paper substrates. Figure 4. 3 is an integrated µPAD (iµPAD) includes the holder, and paper substrates.

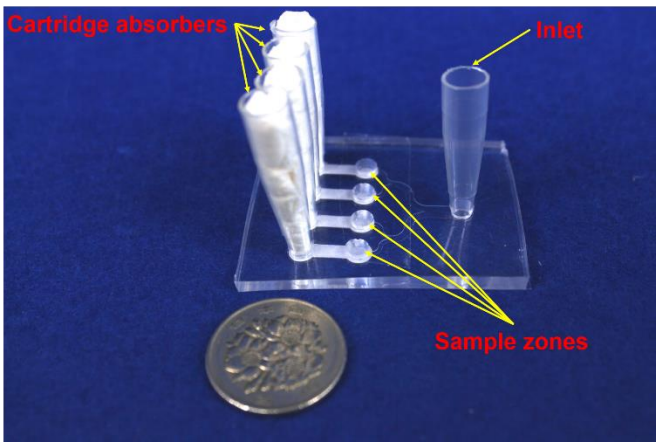


Figure 4. 3 An iμPAD to detect cCys-C.

4.2.3.2 cCys-C assay using the iμPAD

The sample zones were coated with 0.25 mg $mL^{-1}$ dissolved chitosan in 0.1 M HCl for 10 min. Then the chitosan was activated with pipetting 1 μL of 2.5% glutaraldehyde in PBS buffer for 1h. Afterwards, 100 μg $mL^{-1}$ mouse monoclonal anti-cCys-C was pipetted on sample zones (1 μL) and was incubated for 30 min. Then the paper substrates were washed with 0.5% Tween20/PBS (1200 μL). 1% BSA was pipetted into the sample zones to block and prevent non-specific binding of the agents (30 min). After washing the paper substrate as mentioned above, different concentrations of cCys-C was pipetted into the sample zones and incubated for 10 min, separately. Then the paper substrates were washed again to remove unbound agents. Finally, fluorescein-labelled anti-cCys-C was pipetted into the sample zones and incubated for 10 min. After washing the paper substrates, fluorescence images were captured using a fluorescence

microscope and the intensities were measured with AquaCosmos software. All procedures were done at room temperature.

## 4.3 Results and Discussion

### 4.3.1 Detection of cCys-C using microtiter plate and immuno-pillar chips

Detection of cCys-C, as mentioned earlier, has a great potential for application to diagnosis of renal dysfunction of cats in an early stage. We carried out sandwich immunoassays of cCys-C using our immuno-pillar chips and compared the results with those obtained with a conventional ELISA using a 96-well microtiter plate. Each pillar contained about 33000 beads which provided a large surface area to incubate the capture antibody and detect cCys-C with high sensitivity. After incubation with the fluorescence-labelled antibody, we measured the fluorescence intensity. To measure the fluorescence intensity, a circular area of 200 μm diameter was drawn around each pillar using Aqua Cosmos software and average fluorescence intensity was measured. For each 7 concentrations of cCys-C from 0 to 50 ng $mL^{-1}$, the fluorescence intensity of 15 pillars was measured. Standard curves of cCys-C using our immuno-pillar chips and the 96-well microtiter plate are shown in Figure 4. 4. The standard curves had different logistic gradients because the detection methods were different. The fluorescence intensity increased with increasing cCys-C concentration in the immuno-pillar chips and had a good reproducibility ($R^2$= 0.913). The limits of detection (LODs) were calculated as 3 times the standard deviation (SD) of the signal from a blank pillar with zero

cCys-C concentration. The LODs for cCys-C using immuno-pillar chips and the 96-well microtiter plate were 3 ng $mL^{-1}$ and 1 ng $mL^{-1}$, respectively. The higher LOD for the former was because of the higher background signal. However, the cut off value is 1.05 µg $mL^{-1}$ which means the immuno-pillar has enough sensitivity. The absorbance in 96-well microtiter plate also increased with increasing concentration of cCys-C.

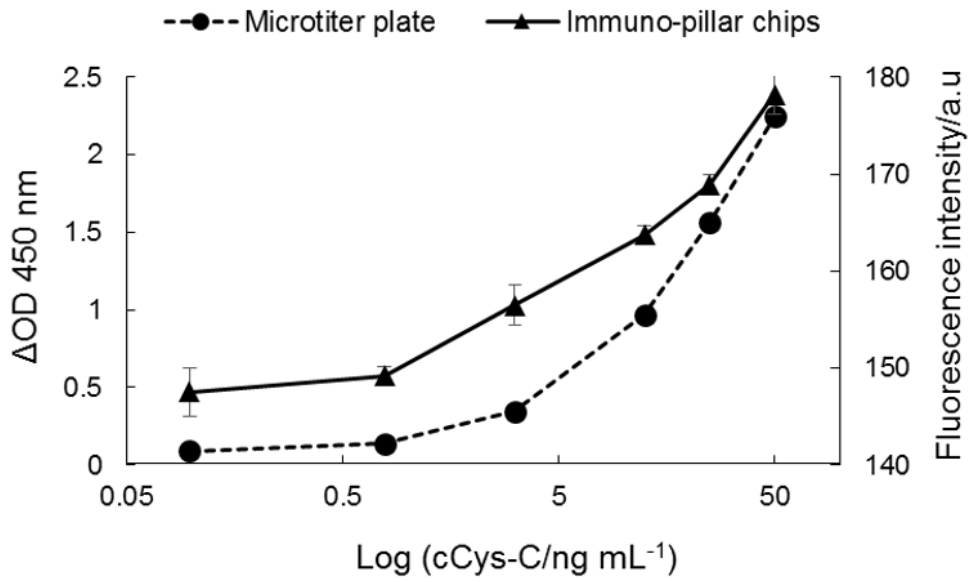


Figure 4. 4 Standard curves for cCys-C using the immuno-pillar chips (solid line with right Y-axis) and microtiter plate (dashed line with left Y-axis).

### 4.3.2 Detection of cCys-C using iµPAD

Fluorescence-labelled antibody was introduced to the sample zones after incubation of different concentrations of cCys-C from 0 to 50 ng $mL^{-1}$. To measure the

fluorescence intensity, a circular area with 2 mm was drawn in centre of the each sample zone using Aqua Cosmos software and average fluorescence intensity was measured. 3 measurements were done for each concentration of cCys-C. A standard curve of cCys-C using our iμPAD is shown in Figure 4. 5. The total time for assay was included the incubation of cCys-C and fluorescence-labelled antibody followed by washing steps in that was 1 h. In addition, because the sample zones were bigger than previous study in the chapter 3 (4.5 vs. 3.5 mm), the reagent consumption was 1 μL in current study. The LOD for cCys-C using iμPAD was 12.5 ng mL $^{-1}$. The cost per assay was estimated regard to cost of reagent of the assay and fabrication of the device.

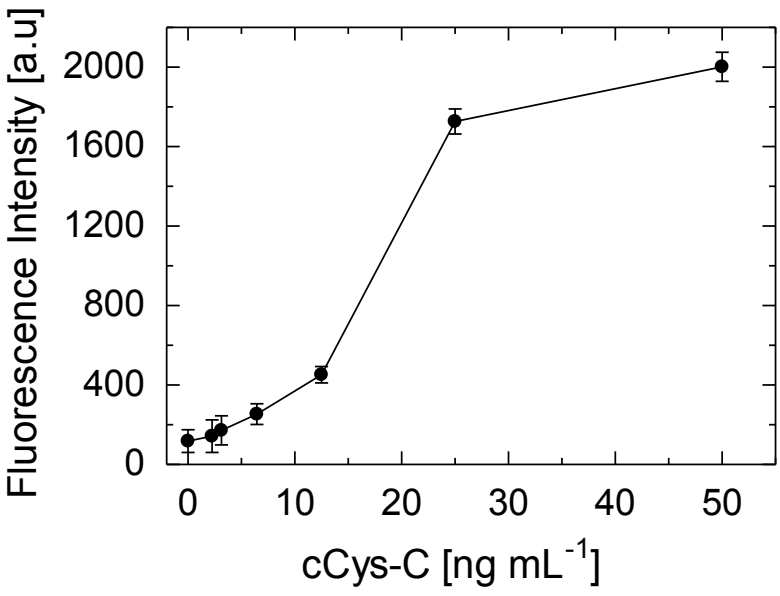


Figure 4. 5 Standard curves for cCys-C using iμPAD.

A comparison of iμPAD with 96 well microtiter plate and immuno-pillar chips is

made in Table 4. 1. In this study, the total assay time included the times for the first and second incubations, washing, and detecting steps; for iμPAD, microtiter plate, and immuno-pillar chips, they were 60, 240, and 20 min, respectively. In addition, reagent consumption was significantly lowered from 100 μL in the 96-well microtiter plate to 0.5 μL in the immuno-pillar chips and 1μL in iμPAD. However, improvement of the LODs in the iμPAD and the immuno-pillar chips (12.5 and 3 ng $mL^{-1}$, respectively) requires further consideration; the 96-well microtiter plate had a LOD of 1 ng $mL^{-1}$.

Table 4. 1 Comparison of iμPAD with 96 well microtiter plate and immuno-pillar chips to detect cCys-C

| Items | iμPAD | microtiter | immuno – pillar chips |
|---|---|---|---|
| Total assay time (min) | 60 | 240 | 20 |
| Volume of reagent (μL) | 1 | 100 | 0.5 |
| LOD (ng $mL^{-1}$) | 12.5 | 0.78 | 3.13 |
| Cost per assay (¥) | 20 | 2500 | 200 |

## 4.4 Conclusion

In this chapter, different methods relying on making a cheaper technique to apply for cCys-C detection were utilized. First of all, cCys-C was detected using conventional 96 wall microtiter plate with limit of detection of 1 ng $mL^{-1}$, However, total assay time was time consuming (240 min) and the assay needed 100 µL of reagents in each step which was expensive. In next attempt, we used immuno-pillar chip which was developed by our group in 2010 to detect cCys-C. We succeed to detect cCys-C in very shorter time than microtiter plate (less than 20 min) by using 0.5 µL of reagents in each step which was significantly declined the cost of the assay, however the sensitivity was lower than microtiter plate (3.13 ng $mL^{-1}$). Finally, we applied the cheapest platform of microfluidic which termed iµPADs to detect cCys-C. The total assay time was 4 times lower than conventional microtiter plate and 3 times longer than the immuno-pillar chips. The LOD for cCys-C detection using iµPAD (12.5 ng $mL^{-1}$) was higher than microtiter plate and immuno-pillar chips but based on the cut of value for cCys-C, iµPAD had acceptable sensitivity. Therefore, iµPAD is recommended as the cheapest and rapid method to detect cCys-C with sufficient sensitivity.

**References**


1. C. L. Marino, B. D. Lascelles, S. L. Vaden, M. E. Gruen and S. L. Marks, J. Feline Med. Surg, 2014, 16, 465-472.
2. S. DiBartola, H. Rutgers, P. Zack and M. Tarr, J. Am. Vet. Med. Assoc, 1987, 190, 1196-1202.
3. D. Paepe and S. Daminet, J. Feline Med. Surg, 2013, 15, 15-27.
4. M. G. Shlipak, K. Matsushita, J. Ärnlöv, L. A. Inker, R. Katz, K. R. Polkinghorne, D. Rothenbacher, M. J. Sarnak, B. C. Astor, J. Coresh, A. S. Levey and R. T. Gansevoort, N. Engl. J. Med., 2013, 369, 932-943.
5. R. Perrone, N. Madias and A. Levey, Clin Chem, 1992, 38, 1933-1953.
6. A. Levey and R. Perrone, N. Madias, Annu Rev Med, 1998, 39, 465-490.
7. O. Shemesh, H. Golbetz and J. Kriss, Kidney Int, 1985, 8, 830-836.
8. M. Rosner and W. Bolton, Am J Kidney Dis, 2006, 47, 174-183.
9. B. Jacobsson, H, Lignelid and U. Bergerheim, Histopathology, 1995, 26, 559-564.
10. P. Nilsson-Ehle, Kidney Int Suppl., 1994, 47, 17-19.
11. V. Dharnidharka, C. Kwon, G. Stevens, Am. J. Kidney Dis., 2002, 40, 221-226.
12. M. Ikami, A. Kawakami, M. Kakuta, Y. Okamoto, N. Kaji, M. Tokeshi and Y. Baba, Lab Chip, 2010, 10, 3335-3340.

13. T. Kasama, M. Ikami, W. Jin, K. Yamada, N. Kaji, Y. Atsumi, M. Mizutani, A. Murai, A. Okamoto, T. Namikawa, M. Ohta, M. Tokeshi and Y. Baba, Anal. Methods, 2015, 7, 5092-5095.

14. N. Nishiwaki, T. Kasama, A. Ishida, H. Tani, Y. Baba and M. Tokeshi, Bunseki Kagaku, 2015, 64, 329-335.

# Chapter 5. Concluding remarks

The results of this thesis can be concluded in three main parts. In the first part fundamental information about fabrication of microfluidic paper-based analytical devices (µPADs) has been studied. Current efforts led to develop a simple, instrument-free, and inexpensive technique to fabricate µPADs by screen-printing of polydimethylsiloxane (PDMS) on chromatography paper. We found that, the minimum hydrophilic channel width that can be fabricated by this method is 600 µm without lack of capillary force of the paper. Furthermore, fabricated µPADs were examined for different colorimetric assays of glucose, protein, and pH titration.

In the second part we considered a new concept for washing of µPADs relying on spontaneous capillary force of the paper substrate. We demonstrated that increasing the permeability of the paper substrate used for multistep assays led to proper removal of unbound agents and decreased the background signal. As an assay model, CRP was detected with the limit of detection of 5 µg $ml^{-1}$. In comparison with the conventional washing technique, the new method developed here for washing of µPADs provided significantly higher sensitivity and reproducibility. By exploiting our washing concept, researchers can be closer to applying µPADs for multistep assays with a low background signal.

In third part, different methods relying on making a cheaper technique to apply for cCys-C detection were utilized. First of all, cCys-C was detected using conventional 96 wall microtiter plate with limit of detection of 0.78 ng $mL^{-1}$, However, total assay time was time consuming (240 min) and the assay needed 100 µL of reagents in each step which was expensive. In next attempt, we used immuno-pillar chip which was developed by our group in 2010 to detect cCys-C. We succeed to detect cCys-C in very shorter time than microtiter plate (less than 20 min) by using 0.5 µL of reagents in each step which was significantly declined the cost of the assay, however the sensitivity was lower than microtiter plate (3.13 ng $mL^{-1}$). Finally, we applied the cheapest platform of microfluidic which termed µPADs to detect cCys-C. The total assay time was 4 times lower than conventional microtiter plate and 3 times longer than the immuno-pillar chips. The LOD for cCys-C detection using iµPAD (12.5 ng $mL^{-1}$) was higher than microtiter plate and immuno-pillar chips but based on the cut of value for cCys-C, iµPAD had acceptable sensitivity. Therefore, iµPAD is recommended as the cheapest and rapid method to detect cCys-C with sufficient sensitivity.

# Acknowledgments

This thesis is results of the author's research for 3 years from October 2013 to September 2016 in Graduate School of Engineering, Hokkaido University. Many people and organizations have been supporting me along the way, and my deepest gratitude goes out to all of them. First of all I would like to express my sincere appreciation to my supervisor Professor Manabu Tokeshi who expertise, understanding, and patience, added considerably to my graduate experience. I doubt that I will ever be able to convey my appreciation fully, but I owe him my eternal gratitude.

Very special thanks go out to Dr. Masatoshi Maeki for providing me with his precious technical advices and his continuous encouragement.

Also I would like to thank Professor Akihiko Ishida for being patience to give his outstanding, helpful guidance along 3 years period of my Ph.D. program.

Special thanks to Professor Hirofumi Tani, Professor Mutsumi Takagi, and Professor Noboru Kitamura for accepting responsibility of being my official co-supervisors.

I must also acknowledge all current and previous members of Professor Tokeshi's group who have been all supportive and kind to me.

Finally I would like to dedicate the literature to my family members, specially my patient and loving wife who has been a great source of strength all through this work.